Understanding (coupled) large amplitude motions: the interplay of microwave spectroscopy, spectral modeling, and quantum chemistry

Ha Vinh Lam Nguyen, Isabelle Kleiner

▶ **To cite this version:**

Understanding (coupled) large amplitude motions: The interplay of microwave spectroscopy, spectral modeling, and quantum chemistry

Ha Vinh Lam NGUYEN[a,*] and Isabelle KLEINER[a]

[a] Laboratoire Interuniversitaire des Systèmes Atmosphériques (LISA), CNRS UMR 7583, Université Paris-Est Créteil, Université de Paris, Institut Pierre Simon Laplace, 61 avenue du Général de Gaulle, F-94010 Créteil, France

* Corresponding author.

Emails: lam.nguyen@lisa.u-pec.fr

isabelle.kleiner@lisa.u-pec.fr

Abstract

A large variety of molecules contain large amplitude motions (LAM), *inter alia* internal rotation and inversion tunneling, resulting in tunneling splittings in their rotational spectrum. We will present the modern strategy to study LAMs using a combination of molecular jet Fourier transform microwave spectroscopy, spectral modeling, and quantum chemical calculations to characterize such systems by the analysis of their rotational spectra. This interplay is particularly successful in decoding complex spectra revealing LAMs and providing reference data for fundamental physics, astrochemistry, atmospheric/environmental chemistry and analytics, or fundamental research in physical chemistry. Addressing experimental key-aspects, a brief presentation on the two most popular types of state-of-the-art Fourier transform microwave spectrometer technology, i.e. pulsed supersonic jet expansion based spectrometers employing narrow-band pulse or broad-band chirp excitation, will be given first. Secondly, the use of quantum chemistry as a supporting tool for rotational spectroscopy will be discussed with emphasis on conformational analysis. Several computer codes for fitting rotational spectra exhibiting fine structure arising from LAMs are discussed with their advantages and drawbacks. Furthermore, a number of examples will provide an overview on the wealth of information that can be drawn from the rotational spectra, leading to new insights on the molecular structure and dynamics. The focus will be on the interpretation of potential barriers and how LAMs can act as sensors within molecules to help us understand molecular behavior in the laboratory and nature.

Keywords: microwave spectroscopy, rotational spectroscopy, large amplitude motions, conformational analysis, spectral fitting, molecular jet Fourier transform

Introduction

Since the jet-based Fourier Transform MicroWave (FTMW) spectroscopy technique was introduced by Balle and Flygare in 1979 [1,2], it rapidly became popular. The complexity of molecules that could be studied strongly increased with this method. In combination with newly developed jet-sources, it shows a great potential towards even larger and more dynamic systems, transient molecules, or weakly bounded complexes with applications in research fields as diverse as, e.g., molecular biology, astrophysics, or environmental sciences.

Rotational spectra have been always known to be related directly to molecular structures, because the most important geometry parameters which they deliver are the rotational constants, which reflect the mass distribution of atoms in the molecules. Information on bond lengths and angles can be routinely obtained. However, microwave spectroscopy is today far more advanced and offers much more than just the molecular structures. It addresses various fundamental and applied problems in molecular physics, physical chemistry, and related fields such as astrophysics, atmospheric sciences, or biochemistry. It answers challenging questions on conformational landscapes, characters of the chemical bond, electronic surrounding of a given nucleus, charge transfer, and internal dynamics.

The power of microwave spectroscopy in decoding molecular structures is very impressive compared to other spectroscopic techniques, because pure rotational transitions can be observed directly within the lowest vibrational state. Furthermore, in combination with supersonic expansion where the rotational temperature is decreased almost to the absolute zero point (from 0.5 to 2 K), only the lowest rotational levels are populated. This leads to a tremendous simplification of the spectra. Although important chemical and spectroscopic information could still be obtained with static gas cells, many problems could only be solved using supersonic jets. At the same time, with the capability to observe spectra of even larger molecules, microwave spectroscopy is emphasizing and

consolidating the key role in yielding accurate information on various physical and chemical objectives. Atmospheric compounds, interstellar species, and biomolecules are targeted in many laboratory studies, which provide information on properties of molecules, clusters, and radicals, as well as offer applications directed toward atmospheric sensing or radio astronomy.

The two classical books known by almost every microwave spectroscopists are Townes and Schawlow [3] and Gordy and Cook [4]. The fundamental theoretical background of rotational spectroscopy is refered to those books and will not be repeated here.

The effects of intramolecular dynamics cause all rotational energy levels to split into several levels due to tunnel effects. Two prototypes of such Large Amplitude Motions (LAMs) are methyl internal rotation and inversion tunneling involving a double minimum potential. These LAMs sometimes complicate the spectra that much that their assignments were inhibited. To model the experimental spectra, theoretical tools including correct Hamiltonian need to be developed. The theory on LAMs occuring in rotational spectra are described in detail by Wollrab [5] and Lister et al. [6], or in reviews, e.g. by Lin and Swalen [7]. Their group theoretical treatment using the permutation inversion group can be found in a book written by Bunker and Jensen [8].
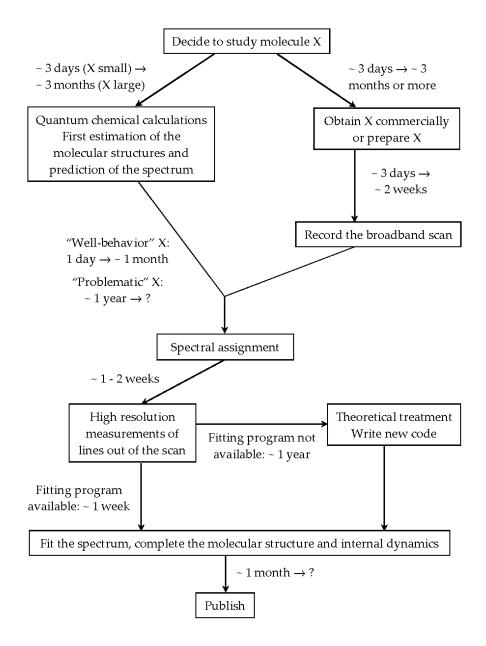
Several computer programs are available to analyze the rotational spectra. They are often developed by microwave spectroscopists during the investigations on their particular molecular systems and then generalized for other molecules with similar molecular symmetry and internal dynamics. Nevertheless, in a number of cases where no program is available to treat the LAM problems occurring in the molecules of interest, specialized codes are needed. They are either extended from an already existing program or written newly. In those cases, group theoretical treatment is required in addition. The rotational spectra of many molecules can be fitted by the program *SPFIT/SPCAT* written by Pickett [9], often used to produce line frequencies and intensities for molecules in the astrophysical databases such as the Jet Propulsion Laboratory (JPL) [10] or ''The Cologne Database for Molecular Spectroscopy'' (CDMS) [11]. Many non-rigid molecules are also

available at other astrophysical line-lists and websites such as Splatalogue [12], the Observed Interstellar Molecular Microwave Transitions NIST database [13], and the Toyama Microwave Atlas [14].

Many programs for rotational spectroscopy dealing with LAMs are available at the ''Programs for ROtational SPEctroscopy'' (PROSPE) managed by Z. Kisiel [15]. Among them, the program *XIAM* written by Hartwig and Dreizler [16] can treat the internal rotation effects of up to three methyl internal rotors. Other codes exist which contain higher order perturbation terms such as the one written by Ohashi and Hougen for methylamine-like molecule [17], by Kleiner and collaborators to deal with a number of one-top [18,19] and two-top molecules [20] with C_s and C_1 symmetry, by Groner to deal with one or two internal tops [21], or by Ilyushin to treat one-top with C_s [22] and two-top molecules with C_{2v} symmetry [23]. Kleiner and Ilyushin use a global treatment including all the torsional levels for a given vibrational state, an approach which is particularly successful for low barriers or excited torsional states. Internal rotations with intermediate to high torsional barriers can be handled by the *IAMCALC* program intergrating in Pickett's *SPFIT/SPCAT* suite [10] and by the spectral fitting program *JB95* provided by Plusquellic [24]. A few models for complicated interactions arising in individual molecules have been also developed based on group theoretical approaches, e.g. studies on the rotatory-wagging coupled motions in 2-methylmalonaldehyde, a methylamine-like molecule, by Kleiner and Hougen using the hybrid model [25].

Density functional theory and *ab initio* calculations implemented in computational programs such as *Gaussian* [26] or *GAMESS* [27] are commonly used today in the spectroscopic community to predict i.a. the potential energy surfaces (PES) to determine the conformational preferences, the molecular equilibrium structures, and electric field gradients. Such calculations yield starting values of spectroscopic parameters including barrier heights for different types of LAMs to support the experimental work.

In the present review, the theoretical or experimental background required to analyze the rotational spectrum of a molecule containing one of more LAMs will not be given in detail, as they were presented in a number of books, papers, and review papers

[3-8]. Instead, this review will summarize the modern strategy to analyze microwave spectra, how to achieve fits with standard deviations within experimental accuracy, and serve as a guideline to study LAM systems, as outlined in Schema 1. Furthermore, it will give an overview how to use the information coming out from the spectrum to bring new insights on the molecular gas phase structures and dynamics. The focus will be on the interpretation of potential barriers and the use of methyl internal rotors as sensors for the molecular structures.

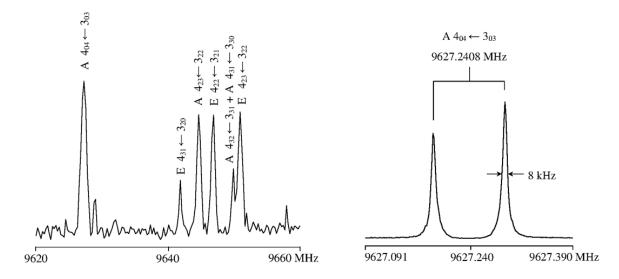**Schema 1.** The general procedure for microwave spectroscopic investigations on a molecular system.

Spectrometer technology

With the unique ability to provide simultaneously high sensitivity and high resolution, FTMW spectroscopy based on pulsed supersonic jet expansions has become popular in the last decades. This technique is a powerful tool for studying isolated molecules in the gas phase. The most attractive advantages of integrating supersonic jet expansion in the FTMW spectrometers is the significant simplification of observed spectra. Furthermore, the signal to noise ratio is increased due to statistical depopulation of the excited states in the molecules because of the effective cooling of the sample to extremely low rotational temperature (0.5 - 2 K). In this review, the two most popular molecular jet FTMW spectrometer techniques will be briefly presented. More details can be found in Ref. [28].

1. Resonator-based molecular jet FTMW (2 − 40 GHz) spectrometers: *High resolution and sensivity but time-consuming for survey spectra*

In a molecular sample, the electric dipole interaction occurs while exposing to a standing wave field of the microwave radiation which propagates in a "transverse electric magnetic"-mode of a Fabry-Pérot-type resonator formed by two spherical mirrors, typically made of aluminum, with equal curvature at a distance d. Today, resonator based molecular jet FTMW spectrometers in the frequency range below 26 GHz are commonly used in many microwave laboratories and have shown their superior sensitivity and resolving power [29-40]. For medium-size or large biomolecules or volatile compounds important for atmospheric chemistry and biology (≥ 15 atoms), this frequency range is suitable because of the small rotational constants. Therefore, lower J and K rotational transitions, which are easier to assign, fall in this range. Spectrometers from 26 to 40 GHz are fairly rare, but extremely useful for studying small molecules (< 15 atoms) abundant in the Earth's atmosphere or in astrophysical objects such as molecular clouds or planetary atmospheres [41].

A diluted gas mixture of about 1% sample seeded in a rare gas at a total pressure in the range of 50 to 200 kPa is expanded into the vaccum chamber which contains the resonators. The simplest form of the nozzle consists of a circular orifice with a diameter of 0.5 – 2.0 mm. The exit channel of the nozzle of 2 mm length is widened conically to 4 mm. The signals appear as doublets due to the Doppler effect in the case of a coaxial arrangement between the resonator and the molecular beam (COBRA-type). The typical measurement accuracy is about 2 kHz. Figure 1 depicts a typical broadband scan and a spectrum recorded at high resolution using a COBRA-type molecular jet FTMW spectrometer [33].

Figure 1. A typical broadband scan (left hand-side) and a spectrum recorded at high resolution (right hand-side) of allyl acetate using a COBRA-type molecular jet FTMW spectrometer [33]. The broadband scan was recorded by overlapping spectra at step size of 0.25 MHz, where only the line positions are present. The linewidth in the high resolution spectrum of the $4_{04} \leftarrow 3_{03}$ rotational transition, A torsional species, is 8 kHz. The line frequency can be determined with a measurement accuracy of about 0.8 kHz [42].

2. Chirped-pulse molecular jet FTMW spectrometers: *How to reduce the time requirements for survey spectra?*

The classical version of resonator-based molecular jet FTMW spectrometers have an unrivalled resolution, but suffer from the time requirement to acquire survey spectra (scans), because the resonator has to be tuned mechanically for every frequency element

at rather narrow steps of less than 0.25 MHz ($< 10^{-5}$ cm^{-1}), see for example the figure caption of Figure 1 [42]. An approach to overcome this problem was developed a decade ago using the chirped-pulse (CP) method, which relies on a very short but powerful frequency-ramp signal with a band width of 1 GHz (3333 times 10^{-5} cm^{-1}) or even more, and thus can reduce the time requirements for scans dramatically [43].
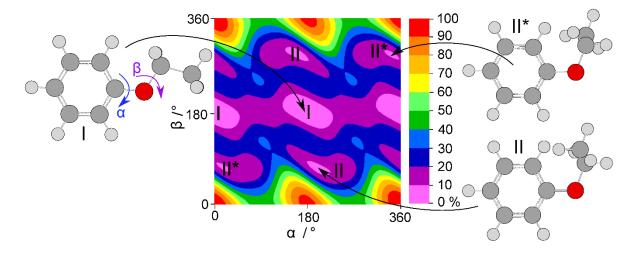
The fast passage excitation arises when the frequency of an electromagnetic field is swept through a molecular resonance in a time which is much shorter than the relaxation time. Despite this very short resonance time, the population of the states changes remarkably, which leads to a detectable oscillating macroscopic polarization. Although traditional narrow-band resonator-based spectrometers can provide better resolution of the spectra of a target molecule, CP-FTMW provides unparalleled speed for highly complex broadband spectra arising from mixtures of reaction products, isomers, or weakly bound molecular clusters. In many studies where optimizations of the molecular jet are required, e.g. van der Waals complexes or electric discharges to produce ions or radicals, the use of a CP machine is indispensable. It is necessary to monitor a wide spectral range in real-time in order to recognize changes in the spectrum while the strength of discharge and other parameters are varied. Furthermore, the line intensities of CP spectra are more reliable than those of a resonator-based apparatus. This is an important feature for assignments of the spectra and for conformational analysis.

With all of these advantages, CP-FTMW is the spectrometer of choice for many scientists worldwide and has been equipped in almost all microwave spectroscopic labs [44-59].

Quantum chemical calculations

The combination of microwave spectroscopy and quantum chemical calculations is a powerful tool to determine the conformational landscape of medium-size and large molecules as well as LAM parameters. Studies where the microwave heavy atom strutures were determined experimentally, such as those on methyltetrahydrofuran [60], 2-ethylfuran [61], and 2- and 3-nitrobenzonitrile [62], have proven that the molecular geometries can be sufficiently well-calculated. In the present review, we constraint the scope of quantum chemical calculations on geometry optimizations. They are crucial and serve as a supporting tool for the assignment of microwave spectra by delivering predicted values to start the assignment [63]. If the molecules are large, it is often not possible to obtain r_s geometries from the experiments, as not all isotopologues can be observed, but geometry information can be indirectly obtained from the rotational constants, which can be compared with those of the theoretical results. Like Townes and Schawlow [3] and Gordy and Cook [4] for microwave spectroscopists, details on quantum chemistry are referred to the two books written by Cramer [64] and Jensen [65]. The present review will only address the use of quantum chemistry as a supporting tool for rotational spectroscopy.

The relation between the positions of all nuclei in a molecule and the corresponding potential of the molecule can be described by the PES. Each energy minimum on the PES represents a stable conformer, because any change in geometry parameters such as bond angles or lengths would lead to a conformation with a higher energy. The absolute miminum is the energetically lowest, i.e. the most favorable, conformation of the molecule. Transition states are also present on the maxima of the PES as saddle points. Figure 2 illustrates the PES of phenetole depending on the rotations of the phenyl ring and the ethyl group as an example [66]. This PES discribes completely the conformational landscape of phenetole.

Figure 2. The PES of phenetole calculated at the MP2/6-311++G(d,p) level of theory obtained by rotating the phenyl ring (dihedral angle α) and the ethyl group (dihedral angle β) [66]. The numbers in the color code indicate the energy (in per cent) relative to the energetic minimum E_{min} = −385.0444525 Hartree (0%) and the energetic maximum E_{max} = −385.02509670 Hartree (100 %). Two energy mimina (I and II) are found on this PES. II* is the enantiomer of II.
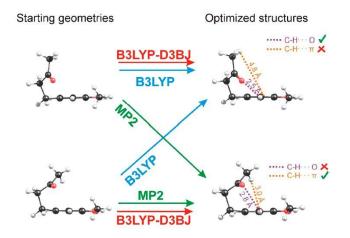
1. Geometry optimizations: *How to start?*

To calculate the stable conformers of a molecule, geometry optimizations are carried out on different starting geometries computed in quantum chemical programs like, for example, the commercially available *Gaussian* [26] or the freeware *GAMESS* [27] where the total energy is minimized by varying the atom positions in small steps until convergence.

As stated in Scheme 1, theoretical investigations can be started immediately after deciding to study a system of interest (called molecule X in Scheme 1), even before the experimental spectrum is recorded. However, several points should be carefully thought before running the first calculation. The first point is to decide which level of theory is most suitable to treat molecule X and how accurate the results will be. The choice of course depends on the available experimental data.
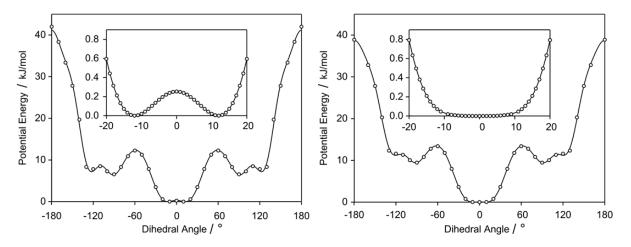
2. Method choice: *Be careful. Discrepancy!*

Different methods are available to optimize the geometry of a molecule and find the stable conformations. The two methods with a reasonable ratio between calculation time and efficiency ratio most commonly used are probably the density functional theory (DFT) using the B3LYP functional [67,68] and the MP2 method [69]. They mainly differ in their optimized quantity. While it is the electron density for DFT, the wave function is optimized by MP2. If the molecule belongs to a systematic investigation on a molecular class, a certain level of theory is often preferred, which has yielded more reliable results in previous studies [70]. Otherwise, MP2 is usually recommended and represents one of the most favorable methods in the microwave spectroscopic community because of the reasonable rate between accuracy and required computational time. However, an advantage of the semi-emperical B3LYP method over the pure *ab initio* MP2 method is that it is much faster and more cost efficient. However, a disadvantage of the B3LYP functional is its underestimation of intramolecular interactions. As a consequence, energy minima may be overlooked during the conformational analysis [71]. This can be improved by using Grimme's dispersion correction [72,73], which turned out to be quite helpful for large molecules containing internal rotation. The case study on methyl jasmonate and zingerone, two substances produced by plants, has shown that a wrong choice of the theoretical method can lead to misinterpretation of experimental results (see Figure 3) [74].

Figure 3. Schematic representation of the prototype behavior of theoretical methods in the conformational casuistry of zingerone. For details see Ref. [74].

The discrepancy between B3LYP and MP2 found in methyl jasmonate and zingerone is not unusual and can also be observed in smaller molecules. An example is the case of diethyl ketone, where MP2 predicts a tilt angle of about 10° for each of the ethyl group and the corresponding symmetry is C_2, while B3LYP calculates a C_{2v} symmetry with all heavy atoms located on the symmetry plane (see Figure 4) [75]. There are also more accurate methods, for example higher orders of perturbation theory (MP4) [76] or the golden standard in quantum chemistry, coupled cluster calculations [77], but they are much more expensive than the B3LYP and MP2 methods. Therefore, a conformational analysis at a level higher than B3LYP or MP2 is not recommended. However, it might be interesting to re-optimize the geometries of the lowest energy conformers obtained from the PES at a higher level to predict more accurate structures.

Figure 4. Left hand side: a potential energy curve of diethyl ketone calculated at the MP2/6-311++G(d,p) level of theory. Right hand side: the same potential curve calculated at the B3LYP/6-311++G(d,p) level of theory. For details see Ref. [75].

2. Basis set choice: *Make a lot of tests…*

The second point is to choose a suitable basis set. The Pople valence triple-zeta basis set 6-311++G(d,p) is often used in combination with the MP2 and B3LYP methods, because the valence shell electrons are described well and the diffuse functions (++) and the polarization function (d,p) are included [78]. A set of polarizing d-functions is used on all atoms heavier than helium and a set of p-functions on all hydrogen and helium atoms is included. Dunning correlation consistent basis sets, e.g. aug-cc-pVDZ and aug-cc-pVTZ

are also often chosen [79]. It is obvious that the same level of theory should be used throughout the conformational analysis for a reasonable comparison.

For each energy minimum harmonic frequency calculations have to be performed to verify whether an optimized geometry on the PES is an energy minimum or a saddle point (transition state). Zero-point energy corrections on the equilibrium energy can also be obtained which yields the energy of the system in the vibrational ground state.

The accuracy of calculations with different methods or basis sets depends on the system of interest X. Therefore, the method/basis set combination should be chosen carefully before running the calculations. A level often used in the spectroscopic community is MP2/6-311++G(d,p), which has provided good starting values in investigations of many small to medium-size molecules [80-82]. The geometries, and consequently the predicted rotational constants, usually agree well with the experimental values. However, the B3LYP/6-311++G(d,p) level of theory turns out to be more reliable in some cases such as the three isomers of mono-methylanisoles [83-85]. For some esters like ethyl valerate [86] or molecules containing aromatic rings such as coumarin [87], quinolone [88], and isoquinoline [88], MP2/6-31G(d,p) turns out to be a "magic level" which calculates rotational constants accidentally closest to the experimental values and has eased significantly the assigment process. It is therefore recommended for any new class of molecules to first test which combination of methods and basis set is appropriate, and then apply it for all following investigations in the series.

Finally, it should be mentioned that the predicted rotational constants refer to the equilibrium structure and the experimental rotational constants obtained from the microwave spectrum are those of the vibrational ground state. Since the deviations are often only about 1%, the theoretical B_e values are usually compared directly with the experimental B_0 results [89]. Though this comparison is not physically meaningful, theoretical B_e values offer cost-efficient calculations with sufficient accuracy for spectral assignment purposes. Theoretical B_0 rotational constants at the vibrational ground state can be provided by anharmonic frequency calculations, which are sometimes important, for example to determine the semi-experimental equilibrium r_e^{SE} structure [90]. However,

for the assignment of microwave spectra, these calculations are firstly, very time-consuming and secondly, often does not predict rotational constants in much better agreement to the experimental values due to error compensation.

3. Estimation of the torsional barriers: *Still challenging*

Barriers hindering the LAMs can be obtained from potential energy scans where the large amplitude motion coordinates are varied in a certain grid while all other geometry parameters are allowed to relax. Though geometry optimizations yield reliable results in many cases, calculating energies still remains a challenge for today's quantum chemistry with even growing computational capacity. Especially, if the energy differences are small, it is difficult to predict the conformers of lowest energy or the barriers of LAMs with a suffisant accuracy to guide the spectral assignment [91]. Although for quantum chemistry, an accuracy of 1 kJ·mol^{-1}, which is approximately 84 cm^{-1}, states energy calculations with high quality, it is far from accurate regarding the experimental requirements. By a change of only one cm^{-1} in the potential barrier, the predicted frequencies can differ hundreds of MHz from the experimental values. However, the order of magnitude is often given correctly and serves as a good orientation for studying the effects of LAMs in the spectrum.

Large amplitude motions

One of the first recorded rotational spectra were probably those of ammonia with its inversion tunneling motion of the nitrogen atom through the plane spanned by the three hydrogen atoms [92]. Ammonia thus exists in two energetically equivalent geometries, which are connected by a tunneling path with the shape of a double minimum potential [4].

The spectra of many molecular systems are dominated by the tunneling splittings of their LAMs. In some cases, two or more LAMs simultaneously generate tunneling splittings, sometimes with Coriolis couplings between them. There are several types of LAMs, but the two most frequent are the internal rotation, typically of methyl groups, and inversion tunneling. The present review does not consider the puckering LAMs of saturated rings and pseudorotation, as occurring for example in tetrahydrofuran [93]. Furthermore, the investigations are limited to isolated molecules and do not consider weakly bound complexes, where complex LAMs also often occur, such as in the methyl glycidate–water complex [94].

A small historical perspective on large amplitude motions

1. Internal rotation

Internal rotation is a LAM where an internal rotor rotates with respect to the rest of the molecule, called the frame. The internal rotor can be symmetric, e.g. a methyl group, or asymmetric, e.g. OH, SH, NH_2 groups. Depending on the symmetry of the rotor and the frame, the number of equivalent minima of the torsional potential can be different.

1.1. Symmetric internal rotor

A threefold potential is present if the internal rotor is a group with C_3 symmetry like the methyl group attached to an asymmetric frame, as described in equation (1) [4]:

$$V(\alpha) = \tfrac{1}{2}V_3(1 - cos3\alpha) + \tfrac{1}{2}V_6(1 - cos6\alpha) + \tfrac{1}{2}V_9(1 - cos9\alpha) \dots \quad\quad (1)$$

The height of this potential, i.e. the V_3 value, can be quite different, from essentially free rotation (almost 0 cm^{-1}) to over 1000 cm^{-1}.

The first internal rotors studied in the microwave domain were often molecules detected in the astrophysical medium. The history of internal rotation is thus closely related to the history of astrophysics detections. *Methanol*, a very important molecule in chemistry and industry, is one of the simplest molecules with hindered internal rotation, with a barrier height of about 380 cm^{-1}, and was therefore studied since a long time by numerous experimental and theoretical investigations, for example by Koehler and Dennison already in 1940 [95]. The structure of methanol has been determined in 1951 by Hughes, Good, and Coles [96]; the millimeter-wave spectrum was investigated by Lees and Baker [97]. The studies were extended by De Lucia et al. in 1989 [98] and then continued by Xu et al. [99].

The barrier to internal rotation of 398(14) cm^{-1} of another astrophysical molecule, *acetaldehyde*, was estimated by Lin and Kilb in 1956 [100]. The spectral analysis was completed later by Bauder [101], Liang [102], and Maes et al. [103]. *Methyl formate*, a further important astrophysical molecule, was studied in the microwave region in 1959 by Curl [104], reporting a barrier to methyl internal rotation of 416(14) cm^{-1}. Later on, Plummer [105], Demaison [106], Oesterling [107], and Oka et al. [108] improved the spectral analysis to great accuracy. *Acetic acid*, a structural isomer of methyl formate, also shows internal rotation [109,110] where the methyl torsional barrier of 174 cm^{-1} was determined in 1957 by Tabor [111] and later improved to be 168.16(17) cm^{-1} by Krischer and Saegebarth [112]. A review of molecules with internal rotation is available in Ref. [113].

1.2. Asymmetric internal rotor

An example among many asymmetric internal rotors is the primary amino group –NH$_2$. The typical example, ethyl amine, for which Fischer and Botskor reported on the spectrum of the *trans* conformer in 1982 [114] and two years later also on the *gauche* conformer [115]. Another interesting example is water, which can also acts as an
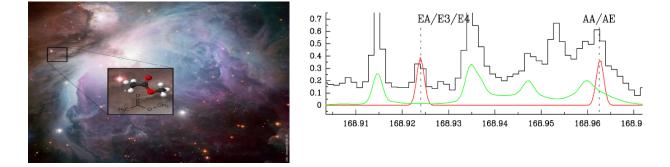
asymmetric internal rotor, causing a V_2 energy potential, as observed in a number of complexes like nitric acid−water [116] or water–carbon oxide [117] or, but we will not consider it further in this review.

1.3. Why is internal rotation important?

The smaller the barrier to internal rotation is, the larger are the splittings in the spectrum [4], and the more complicated is the spectrum analysis. Why should we care about the laboratory analysis of those spectra? One reason is to understand the molecular structure itself which can be used to study chemical and biochemical intrinsecal properties. With increasing sensivity in atmospheric detection, internal rotors have been frequently observed and play an even more important role in the chemistry of the earth atmosphere though they are present only in traces as volatile organic coumpounds. Another reason is that knowledge about internal rotation is essential for the detection of molecules in the interstellar medium. More than 200 molecules have been found in the circumstellar shells or interstellar medium. A number of them show methyl internal rotation with observable splittings. The classical example is methanol, one of the simplest molecules showing methyl internal rotation with a barrier height of about 380 cm^{-1}, which was detected in Orion-A by Lovas et al. in 1976 [118]. About at the same time, Churchwell and Winnerwisser found methyl formate in Sgr B2 with the A-E doublet of the $1_{10} \leftarrow 1_{11}$ transition [119]. Acetaldehyde was also found in Sgr B2 [120], and then in two other clouds TMC-1 and L134N [121]. Acetic acid was first detected in the ISM by Mehringer et al. [122]. Many internal rotor molecules were observed in Orion-KL such as dimethyl ether [123]. Larger molecules like acetone [124] and ethyl methyl ether [10] have been detected as well. Most of the identifications were enabled by the interplay between laboratory studies of the rotational spectra and observations of interstellar surveys in the microwave, sub-millimeter wave, and millimeter wave frequency ranges. The laboratory investigations yield reliable data such as line lists and intensity needed for the interpretation of interstellar survey.

Only a few years ago, 215 unblended lines as well as 163 lines moderately blended with other species of *methyl acetate* with its five torsional splittings arising from two

inequivalent methyl rotors were detected in the Orion cloud [126]. The detection is fully secured taking into account (i) the large number of detected lines and (ii) the fact that the systematic pattern of the lines arising from the different internal rotation states is always present (Figure 5). This success was due to the laboratory work and understanding of the molecular transitions occurring in the microwave spectra of a two-top internal rotor.
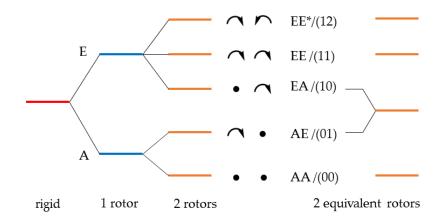

Figure 5. Selected lines (in red) of methyl acetate, CH_3COOCH_3, at 2 mm toward Orion-IRc2. The lines from the different torsional states are identified. The continuous green line corresponds to all lines already modeled from Ref. [126].

1.4. Understanding two-top molecules towards astrophysical detections

All rotational lines of a one-top molecule split into an A and an E torsional component. As illustrated in Figure 6, in the case of *two non-equivalent* internal rotors, all A components split into the so-called AA-AE doublets, and all E components into the EA-EE-EE* triplets, according to the notation by Dreizler based on the direct product $C_{3v}^{(1)} \otimes C_{3v}^{(2)}$ [127]. In the spectra of molecules with *two equivalent rotors*, AA-AE-EE-EE* quartets arise instead of quintets due to the degeneracy of the AE and EA torsional components (see Figure 6). Filled circles in Figure 6 indicate the non-rotating state of the rotors and round arrows symbolize the two rotating states. If the molecular symmetry of the rest of the molecule excluding the methyl groups (so-called the "frame") is C_s, new labeling schemes using the semi-direct products have been introduced for both, the two inequivalent and two equivalent rotor cases. The torsional species are denoted as (00), (01), (10), (11), and (12) [128], where (01) = (10) in equivalent rotor cases [129]. The molecular symmetry groups are G_{36} and G_{18}, respectively. Laboratory studies on the smallest acetate,

methyl acetate, first by Sheridan and Bauder [130], then by Tudorie *et al.* [20] and Nguyen *et al.* [131], and the understanding of molecular energy levels have eventually provided reliable line lists and line intensities for the succesful search and unambiguous detection of this molecule in the Orion cloud, as shown in Figure 5 [126].

Figure 6. Splittings due to internal rotation in the rotational spectrum of molecules with one rotor, two non-equivalent rotors, and two equivalent rotors.

There are also some other investigations on two inequivalent top C_s molecules such as 2-acetyl-5-methyl-furan [132], ethyl methyl ketone [133], methyl propionate [134], dimethylbenzaldehydes [135], dimethylanisoles [128,136,137], and 4-methylacetophenone [138], but the number is still scarce. To our knowledge, so far only one molecule with two inequivalent tops and C_1 symmetry for the frame, isopropenyl acetate, was reported in the literature [139]. The spectra show splittings arising from a low barrier internal rotation of the acetyl methyl group (135.3498(38) cm^{-1}) and a high barrier hindered rotation of the isopropenyl methyl group (711.7(73) cm^{-1}).

For two equivalent methyl internal rotors, only a handful of molecules like acetone [140], dimethyl ether [141], dimethyl diselenide [142], diethyl ketone [75], 2,5-dimethylfuran [143], 2,5-dimethylthiophene [129], and dimethyl sulfide [144] were reported in the literature.

1.5. Beyond two internal rotors

Considerably fewer molecules with more than two methyl internal rotors such as trimethyl silyl iodide, $(CH_3)_3SiI$ [145] and similar systems [146] and *N,N*-dimethylacetamide [147] have been studied. The number of methyl tops is three in all cases. In *N,N*-dimethylacetamide, interactions between the methyl internal rotations and the overall rotation were characterized by Coriolis-like coupling parameters, which allowed the determination of the torsional barrier heights to be 677 cm^{-1} for the C-methyl top, 237 cm^{-1} for the *trans-N*-methyl top, and 183 cm^{-1} for the *cis-N*-methyl top [147].

2. Inversion tunneling

An well-known inversion process is the case of ammonia, NH_3, with a double minimum potential tunneling pathway [92]. Nevertheless, this effect is not only found there but also in larger and more complex molecules.

In an investigation on ***ethylene diamine***, NH_2–CH_2–CH_2–NH_2, Marstokk and Møllendal reported two conformers, in both of which tunneling LAMs occurred when the amino groups interchanged their donor and acceptor roles [148]. Separately fitting the (+) and (−) energy levels yielded quite different inversion splittings of 1.564(66) MHz and 86.356(21) MHz and for the two conformers. After theoretical improvements, a global fit could be achieved by Merke and Coudert [149]. ***Hydrazine***, NH_2–NH_2, is another molecule possessing two amino groups, where three LAMs simultaneously occur, namely an internal rotation about the N−N bond and the inversion motions asiring from both amino groups. The rotational spectrum of hydranzine was first assigned by Kasuja et al. [150] and then improved by Tsunekawa, Kojima, and Hougen [151] as well as by Kreglewski et al. in the sub-millimeterwave range [152] and in the infrared range [153,154]. Inversion tunneling was also observed in almost all primary amines such as aniline C_6H_5–NH_2 [155].

Tunneling motion is also linked to many complexes like dimers as the weak van der Waal bonds are usually quite "floppy". In a theoretical study, Ohashi and Hougen suggested 25 tunneling motions which might occur in methanol dimers in addition to the internal rotations of the two methyl groups [156]. The group theoretical results had been confirmed by the experiments where Lovas et al. revealed in the microwave spectrum 15

different tunneling states of the *a*-type *R*-branch $K_a = 0$ rotational transitions [157]. While a considerable number of studies on molecules with internal rotations are available, investigations on inversion tunneling are scarce. Furthermore, this effect is often combined with internal rotation(s). An example is the inversion of the two protons in the amino group found in primary amines, which is accompanied by the internal rotation of the entire amino group. Only in a few molecules like planar secondary amines such as dimethyl amine, CH_3−**NH**−CH_3, [158] ethyl methyl amine, CH_3−CH_2−**NH**−CH_3, [159] and diethyl amine CH_3−CH_2−**NH**−CH_2−CH_3, [160] the inversion tunneling of the proton is not coupled with internal rotations (though small splittings from methyl torsions can be resolved). In phenyl formate, the tunneling of the phenyl ring also represents the only LAM of this molecule [161].

3. Interaction of internal rotation(s) with tunneling motion(s): *from rotation-wagging to hydrogen transfer*

One of the classical example is the coupling between the methyl internal rotation and the inversion motion of the amino group in ***methyl amine***, where the back-and-forth motion of the amino group triggers a 60° corrective rotation of the methyl group, thereby resulting in six energetically equivalent molecular framworks. The coupling of inversion, vibration, and torsion states of methyl amine has been studied by Gulaczyk, Kreglewski, and Horneman in the infrared spectral range [162,163] and more recently the excited torsional states in the far-infrared range [164].

Another interesting example where a methyl internal rotation interacts with another LAM, the proton tunneling, is ***2-methylmalonaldehyde***. Similar to the case of malonaldehyde, the hydrogen transfer in 2-methylmalonaldehyde is accompanied by tautomeric rearrangements of single and double bonds [165], but the additional consequence is a rotation of the methyl group by 60°. Chou and Hougen [166] developed a tunneling-rotation Hamiltonian based on the G^{12}_m molecular symmetry group to perform global fits of several isotopologues with root-mean-square deviations close to measurement accuracy [167].

The microwave spectrum of ***pinacolone*** also caused surprises with splittings arising from the acetyl methyl group in A-E doublets coupled with the oscillation LAM of the *tert*-butyl group with splittings into the v_t = 0 and 1 states [168]. The same problems occur in the spectrum of acetanilide [169], where the internal rotation of the acetyl methyl group interacts with the tunneling motion of the phenyl ring, which is tilted out of the acetyl plane and a double minimum potential is present. Probably, there are more cases where such coupled LAMs are observed, but the number of publications on those systems are still very limited. According to Scheme 1 in the Introduction section, such "problematic" molecules require extensive measurements and spectral analysis, as well as very often new program code to fit their spectra. All of these usually inhibit the way to publication. On the other hand, they are ideal systems for the development of new group theory as well as for testing the Hamiltonian and theoretical models.

Spectral modeling

1. Global fits of rotational spectra with LAMs: *The way to achieve standard deviations within experimental accuracy*

Treating the microwave spectrum of a rigid rotor is a classical approach where a rigid rotor Hamiltonian H_r supplemented by centrifugal distortion terms H_{CD} is sufficient for a fit of high quality. Many programs are available to treat rigid rotor rotational spectra, considering even higher J and K transitions as well as several vibrational excited states. The programs most frequently used in the high resolution spectroscopic community for this type of molecules are probably *SPFIT/SPCAT* [9], *XIAM* in its rigid rotor mode [16], *JB95* [24], *AUTOFIT* [170], etc. A number of softwares for rigid or non-rigid molecules are available with examples of input/output files at the PROSPE website [15].

The microwave spectrum of a molecule undergoing methyl internal rotation features splittings of each rotational transition into torsional components, and can no longer be treated using a rigid rotor model. In comparison to the large number of rigid rotor programs, only a few programs have been developed to deal with the effects of internal rotations.

1.1. The *SPFIT/SPCAT (IAMCALC)* package

A fitting and prediction program which is very convenient and familiar to many spectroscopists is the *SPFIT/SPCAT* package of Pickett with addition of the front-end program *IAMCALC* [10], as described the case of propane, a two-top molecule with high torsional barriers [171]. The Mathieu function was used to generate a set of parameters connecting torsional sublevels (v_t = 0, 1, 2, A, E). The theoretical model takes into account interactions between the lowest torsional states. This package is also often used in the astrophysical communties, as well as in the JPL [10] and CDMS databases [11].

1.2. The *XIAM* code

Another program popularly used to model rotational spectra with spittings arising from up to three symmetric internal rotors, typically methyl groups, is *XIAM*, written by Hartwig [16]. Geometry parameters like the rotational and centrifugal distortion constants as well as internal rotation parameters such as the V_3 and higher potential terms, the angles between the internal rotor axes with the principal axes, the moment of inertia of the internal rotors, some top-top potential and kinetic coupling terms can be fitted. In addition, *XIAM* uses a first order approximation to treat the hyperfine structures arising from nuclear quadrupole interactions of one nucleus. The fit quality is often quite satisfactory in the cases of nuclei with small quadrupole moments such as ^{14}N.

The rigid frame-rigid top Hamiltonian for an asymmetric molecule with a methyl top in the principal axis system can be written as:

$$H = AP_a^2 + BP_b^2 + CP_c^2 + F(p_\alpha - \rho_a P_a - \rho_b P_b - \rho_c P_c)^2 + V(\alpha) \tag{2}$$

Where P_g ($g = a, b, c$) are the components of the total rotational angular momentum and p_α is the internal rotation angular momentum associating with the torsion angle α. The relations between the rotational constants *A, B, C* of the molecule, the rotational constant *F* of the internal rotor, and the ρ_g components of the ρ vector to the principal moments of inertia I_g of the molecule and to the moment of inertia of the top I_α can be expressed as:

$$A = \frac{\hbar^2}{2I_a}, \ B = \frac{\hbar^2}{2I_b}, \ C = \frac{\hbar^2}{2I_c}, \ F = \frac{\hbar^2}{2rI_\alpha}, \ \rho_g = \frac{\lambda_g I_\alpha}{I_g}, \ r = 1 - \sum_g \lambda_g^2 \frac{I_\alpha}{I_g} \tag{3}$$

where $\lambda_g = \cos \angle(i, g)$ are the direction cosines of the internal rotation axis *i* of the top.

The program *XIAM* uses a combined axis method where the internal rotation problem is first set up in the principal axis system. For each individual internal rotor, the Hamiltonian matrix is transformed into a rho axis system to eliminate the Coriolis coupling terms which occur in Eq. (2). In the rho axis system, the eigenvalues are calculated in the product basis of planar rotor functions for the torsion and symmetric top

functions for the overall rotation. Subsequently, the eigenvalue matrix is transformed back to the principal axis system.

The *XIAM* code is very user-friendly and offers a reasonable compromise of accuracy and speed of the calculations because of suitable basis transformations and matrix factorization. Therefore, it rapidly became one of the programs most frequently used to fit rotational spectra of many molecules where internal rotations take place. However, a known weakness of *XIAM* is the treatment of methyl torsions with low barrier heights, for example in 3-pentin-1-ol [172], vinyl acetate [173], and *N*-ethylacetamide [174], where in the fits standard deviations within measurement accuracy cannot be achieved.

1.3. The *BELGI* code

The program *BELGI*, initially written by Kleiner, Hougen, and Godefroid, is also popularly used to deal with internal rotation problems [18]. The Hamiltonian is written in the Rho Axis Method (RAM):

$$H_{RAM} = H_r + H_{CD} + H_T + H_{int} \tag{4}$$

where H_r is the rotational Hamiltonian, H_{CD} is the centrifugal distortion Hamiltonian, H_T is the torsional Hamiltonian, and H_{int} consists of higher order torsional-rotational interaction terms:

$$H_R = A_{RAM}P_a^2 + B_{RAM}P_b^2 + C_{RAM}P_c^2 + D_{ab}(P_aP_b + P_bP_a),$$

$$H_T = F(p_\alpha - \rho P_a)^2 + V(\alpha). \tag{5}$$

D_{ab} is an out-of-plane parameter arising from the use of a non-principal system. The relation between the rotational constants *A*, *B*, *C* in the principal axis system given in Eq. (2) and the constants in the rho axis system in Eq. (5) is obtained by diagonalizing the 3x3 matrix of the RAM rotational constants [175].

There are two versions of *BELGI* for molecules with a Cs frame symmetry, *BELGI-Cs* for one internal rotor [18] and *BELGI-Cs-2Tops* for two internal rotors of C3v symmetry [20], as well as BELGI-C1 for one rotor and a C1 frame symmetry [19]. *BELGI-Cs* was tested extensively on acetaldehyde [176,177]. Later, spectra of other molecules like acetic acide

[178,179] and ^{13}C-methyl formate (H[13]COO–CH$_3$) [180] were treated with this program as well. The *BELGI-C$_s$-2Tops* code was applied to methyl acetate [20,131], ethyl methyl ketone [133], methyl propionate [134], and dimethylbenzaldehyde [135]. Unlike *XIAM*, *BELGI-C$_s$* and *BELGI-C$_1$* use only the rho axis method.

The program *BELGI* in its recently developed hyperfine versions *BELGI-C$_s$-hyperfine* and *BELGI-C$_1$-hyperfine* [184] as well as *BELGI-C$_s$-2Tops-hyperfine* [185] includes weak nuclear quadrupole coupling using a first order perturbation approximation and has proved its predictive power for a number of molecules such as *N-tert*-butylacetamide (C$_s$, one-top) [184], *N*-ethylacetamide (C$_1$, one-top) [174,184], 3-nitrotoluene (C$_s$, one-top) [186], and 4,5-dimethylthiazole [185].

1.4. The *RAM36* code

Similar approaches are utilized by the program *RAM36*, written by Ilyushin and collaborators, currently existing in a version for fitting a V_6 potential with its application on e.g. toluene [22] as well as 3,5- and 2,6-difluorotoluene [181]. The combination of ^{14}N quadrupole coupling and methyl internal rotation can be handled with the program *RAM36*, but so far only for molecules with C$_s$ symmetry, for example in the case of nitromethane with a V_6 potential [182] or *N*-methylformamide with a V_3 potential [183]. *RAM36* is very fast and uses a procedure which allows the user to choose various higher order terms and to achieve fits for very high J values.

1.5. The *ERHAM* code

A futher program often applied to treat rotational spectra of molecules with up to two internal rotors and J_{max} = 120 is *ERHAM*, written by Groner [21]. The C$_{3v}$ symmetry of internal rotors restricted in *XIAM* and *BELGI* does not applied for *ERHAM*. In molecules with one rotors or two non-equivalent rotors, the frame symmetry can be C$_s$ or C$_1$, as well as C$_2$, C$_{2v}$, or C$_s$ for two equivalent rotor cases. The physical meaning of the fitted parameters is not as clear as in *XIAM*, *BELGI*, or *RAM36*, as *ERHAM* sets up and solves an **E**ffective **R**otational **HAM**iltonian. For example, the rotational barrier is not a fit parameter and needs to be extracted. On the other hand, *ERHAM* is very fast and therefore

advantageous in fitting large data sets. The fit quality is usually quite satisfactory with standard deviation close to experimental accuracy. Dimethyl ether was the first molecule fitted by *ERHAM*, first by its author [187] and then by Endres et al. [188] Another two-top molecule with equivalent rotors, acetone, was also extensively studied with *ERHAM* [140]. A large number of one-top molecules were treated by *ERHAM*, such as methyl carbamate [189], pyruvic acid [190], methyl formate [191], pyruvonitrile [192], methyl isobutyl ketone [193], as well as molecules with two inequivalent rotors like isopropenyl acetate [139].

1.6. The *PAM-C$_{2v}$-2tops* code

A further program written explicitly for molecules with two equivalent methyl rotors and a C$_{2v}$ symmetry at equilibrium is *PAM-C$_{2v}$-2tops*, written by Ilyushin and Hougen. *PAM-C$_{2v}$-2tops* was applied first to acetone [23,194], then to 2,5-dimethylfuran [143]. It uses a two-dimensional potential function and can fit rotational transitions of different torsional states simultaniously. Under group theoretical considerations, the program is based on the G$_{36}$ permutation-inversion group. *PAM-C$_{2v}$-2tops* utilizes the principal axis method and applies a two-step diagonalization procedure. The two-top torsion-rotational Hamiltonian matrix under the full G$_{36}$ permutation-inversion group is split into four submatrices under the G$_9$ permutation-inversion group, corresponding to the (00), (01), (11), and (12) symmetry species, for blockwise diagonalization. These (00), (01), (11), and (12) blocks represent the (A$_1$ $\oplus$ A$_2$ $\oplus$ A$_3$ $\oplus$ A$_4$), G, (E$_3$ $\oplus$ E$_4$), and (E$_1$ $\oplus$ E$_2$) symmetry species in G$_{36}$, respectively.

2. Separate fits of LAM species: *Quick check of the assignments*

With the use of supersonic expansion, torsional symmetry species in the vibrational ground state ($v_t = 0$) can be observed. The excited states are no longer populated because of the very low rotational temperature of the jet. Consequently, it is often not possible to determine the contributions of higher order terms (V_6, V_9…) in the potential function of Eq. (1). Simultaniously fitting the potential terms and moments of inertia of the internal rotors often fails. It is also difficult to determine the potential or kinetic coupling terms in the

case of coupled internal rotors. Cheking the assignments and finding new lines become very difficult and time-consuming tasks using a global fit. For these purposes, fitting the different symmetry species separately and treating them as individual species without any coupling with each other turn out to be helpful. This is a method which is known to work usually well for the A species where a semi-rigid rotor Hamiltonian supplemented by centrifugal distortion corrections, $H = H_r + H_{CD}$, is sufficient to obtain a fit with standard deviation close to the measurement accuracy, even for molecules where the barriers to methyl internal rotation are lower than 10 cm^{-1}, such as 3-pentyn-1-ol (fit A in Table 2 of Ref. [172]).

By adding effective terms in the Hamiltonian, taking into account the E species lines, and using a model including a number of interactions within the torsional bath, a stardard deviation close to measurement accuracy of 2 kHz can be achieved. In the above mentioned example on 3-pentyn-1-ol, the global fit was performed with the program *BELGI-C₁* with a standard deviation of 1.5 kHz [172]. However, such global fits only work with relatively well-assigned data sets. The initial assignment of torsional excited species (E species for one-top molecules, (01), (10), (11), and (12) for two-top molecules and so on) is often performed with the program *XIAM*. This procedure is very time-consuming and uncertain because of the large standard deviation of the *XIAM* fit, especially for low barrier cases. Furthermore, with more than two rotors, no effective Hamiltonian programs are available to check the assignment. Checking the asssignments with combination difference loops is not always possible.

2.1. Test case 1: *A very low barrier (10 cm^{-1}) with C₁ symmetry*

The question to be addressed is how to get a good prediction for all torsional species to ease the assignment purpose. As mentioned, this works well for the torsional ground state (A or (00) species and so on) which can be fitted separately with $H = H_r + H_{CD}$. However, such separate fit can be done for any other symmetry species if angular momentum operators of odd power, e.g. P_a , P_b, $P^2 P_a$, are included in the Hamiltonian. A computer code, called "Separately Fitting Large Amplitude Motion Species (*SFLAMS*)",

was written for this purpose [138]. The main part of the Hamiltonian of Eq. (2) implemented in *SFLAMS* has the form:

$$H = AP_a^2 + BP_b^2 + CP_c^2 + Q_a pP_a + Q_b pP_b + Q_c pP_c \qquad (6)$$

where all terms are even order. If the $Q_a p$, $Q_b p$, and $Q_c p$ terms are substituted by the expectation value $\langle E|p|E \rangle$ of p and become Q'_a, Q'_b, Q'_c, the power of some terms in the Hamiltonian becomes odd. The expectation value is obviously zero for the A species. A similar approach was applied in the program *JB95* [24] and a program written by Ohashi to fit separately the five torsional species of *N*-methylacetamide [195]. Under the time-reversal operation, the odd power terms of the angular momentum components P_a, P_b, and P_c change sign. The Q'_a, Q'_b, Q'_c coefficients enclose numerical expectation values of an odd power of the torsional angular momentum operators of the methyl group (p_α), making the torsion-rotational Hamiltonian effective. Nevertheless, p_α would also change sign under time reversal as the odd power P_a, P_b, and P_c operators did if they were included explicitly in the Hamiltonian. The cancelation of sign changes makes the Hamiltonian invariant as it should be.

Coming back to the example on 3-pentyn-1-ol mentioned above: While the program *SFLAMS* was applied, the standard deviation of 2.3 kHz was obtained for 51 A species lines by fitting only the three rotational and five quartic distortion constants. A similar standard deviation of 3.2 kHz could be obtained for 36 E species lines by adding the *q*, *r*, and *s* parameters, which are Q'_a, Q'_b, Q'_c, respectively, in Eq. (6) and some higher odd order parameters such as q_J, q_{JK}, r_K etc. (see Table 1).

2.2. Test case 2: *A four-top molecule*

The use of *SFLAMS* is best demonstrated in the case of 2,3,4,5-tetramethylthiophene, a molecule featuring four methyl rotors, two of which are in close proximity to the sulfur atom and are equivalent, the other two are also equivalent (see Figure 7). Group theoretical treatment has shown that there are 25 torsional species for this molecule, among them 13 species could be assigned [196]. A typical spectrum is illustrated in the left hand-side of

Figure 8. No global fit could be made due to the lack of suitable program. Separate two-top and three-top fits were carried out with the program *XIAM*, but the results of all those fits are not sastisfactory as they do not reach the experimental accuracy [190].

Table 1. Molecular parameters of the A and the E species of 3-pentyn-1-ol obtained with the program *SFLAMS*.

<table>
<tr><td colspan="3">**3-pentyn-1-ol A**</td><td colspan="4">**3-pentyn-1-ol E**</td></tr>
<tr><td>**Par.[a]**</td><td>**Unit**</td><td>**Values[b]**</td><td>**Par.[a]**</td><td>**Unit**</td><td>**Values[b]**</td><td>**Operator[c]**</td></tr>
<tr><td>A</td><td>MHz</td><td>8.45793216(76)</td><td>A</td><td>GHz</td><td>8.39348(24)</td><td>P_a^2</td></tr>
<tr><td>B</td><td>MHz</td><td>1.68514419(72)</td><td>B</td><td>GHz</td><td>1.6843810(23)</td><td>P_b^2</td></tr>
<tr><td>C</td><td>MHz</td><td>1.46706317(70)</td><td>C</td><td>GHz</td><td>1.4674993(45)</td><td>P_c^2</td></tr>
<tr><td>D_J</td><td>kHz</td><td>0.8730(32)</td><td>D_{JK}</td><td>kHz</td><td>44.16(67)</td><td>P^4</td></tr>
<tr><td>D_{JK}</td><td>kHz</td><td>−4.524(19)</td><td>D_K</td><td>MHz</td><td>−0.680(66)</td><td>$P^2P_a^2$</td></tr>
<tr><td>D_K</td><td>kHz</td><td>56.48(18)</td><td>d_1</td><td>MHz</td><td>−0.09318(62)</td><td>P_a^4</td></tr>
<tr><td>d_1</td><td>kHz</td><td>0.20637(51)</td><td>q</td><td>GHz</td><td>14.834780(97)</td><td>P_a</td></tr>
<tr><td>d_2</td><td>kHz</td><td>5.57(34)</td><td>q_J</td><td>kHz</td><td>−20.97(67)</td><td>P^2P_a</td></tr>
<tr><td>N^d</td><td></td><td>51</td><td>q_{JK}</td><td>kHz</td><td>−1.900(19)</td><td>$P^2P_a^3$</td></tr>
<tr><td>rms^e</td><td>kHz</td><td>2.3</td><td>q_K</td><td>MHz</td><td>−1.53(22)</td><td>P_a^3</td></tr>
<tr><td></td><td></td><td></td><td>r</td><td>GHz</td><td>1.20349(10)</td><td>$P_+ + P_-$</td></tr>
<tr><td></td><td></td><td></td><td>r_J</td><td>kHz</td><td>−8.10(13)</td><td>$P^2(P_+ + P_-)$</td></tr>
<tr><td></td><td></td><td></td><td>r_K</td><td>MHz</td><td>1.093(78)</td><td>$\{P_a^2, (P_+ + P_-)\}$</td></tr>
<tr><td></td><td></td><td></td><td>r_{KK}</td><td>MHz</td><td>−0.2506(51)</td><td>$\{P_a^4, (P_+ + P_-)\}$</td></tr>
<tr><td></td><td></td><td></td><td>s</td><td>GHz</td><td>0.192863(23)</td><td>$P_- - P_+$</td></tr>
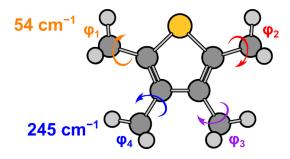<tr><td></td><td></td><td></td><td>N^d</td><td></td><td>36</td><td></td></tr>
<tr><td></td><td></td><td></td><td>rms^e</td><td>kHz</td><td>3.2</td><td></td></tr>
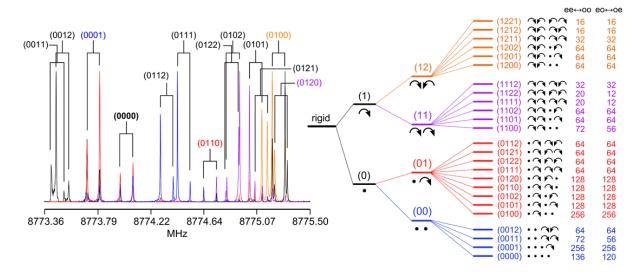</table>

[a] Watson's S reduction and I^r representation were used. [b] Standard errors in parentheses are in the units of the last digit. [c] The product of the parameter and operator from a given row yields the term actually used in the Hamiltonian. [d] Number of line. [e] Root-mean-square deviation of the fit.

Using *SFLAMS*, the torsional species are fitted well separately with standard deviations close to measurement accuracy. From the q and r parameters, the symmetry species could be unambiguously assigned. For example, the q and r values of the (0101) species should be the sum of the q and r values of the (0001) and (0100) species for each

parameter (see Table 2). A small deviation occurs because this sum rule does not take into account the higher order terms connecting to q and r.

Figure 7. The four-top molecule 2,3,4,5-tetramethylthiophene. The two upper tops φ_1 and φ_2 as well as the two bottom tops φ_3 and φ_4 are equivalent [190]. The preliminary torsional barriers are given.

Figure 8. Left hand-side: Splittings due to internal rotation in the rotational spectrum of 2,3,4,5-tetramethylthiophene with two pairs of equivalent rotors. Right hand-side: Spin statistical weights of the allowed b-type transitions [190].

SFLAMS and all effective programs fitting separately the torsional states yield very precise predictions for spectral assignment purposes. Extracting the barrier heights from the q, r, and (if allowed by symmetry) s parameters or vice versa is possible, however is currently performed manuelly and only for certain one-rotor cases. The use of global approaches taking all states into account simultaneously and allowing a direct

determination of the potential barrier is thus complementary to this so-called "local" approach.

Table 2. The rotational constants, q, r parameters, and the root-mean-square deviations of some assigned species of 2,3,4,5-tetramethylthiophene obtained with the program *SFLAMS* [138].

		(0000)	(0001)	(0011)	(0012)	(0100)
A	GHz	1.831412151	1.831174074	1.830935893	1.830936122	1.816106857
B	GHz	1.386904417	1.386632349	1.386359251	1.386359726	1.385709333
C	GHz	0.800078070	0.800078483	0.800078536	0.800078238	0.800110164
q	MHz	0.0	19.6	0.0	39.3	1224.3
r	MHz	0.0	22.4	44.9	0.8	285.9
rms	kHz	2.6	2.7	1.8	1.4	1.2

		(0101)	(0110)	(0111)	(0120)
A	GHz	1.815876903	1.815838209	1.815602766	1.815863307
B	GHz	1.385426931	1.385433503	1.385150624	1.385429503
C	GHz	0.800110910	0.800111933	0.800110473	0.800110210
q	MHz	1244.9	1205.4	1226.1	1246.3
r	MHz	309.9	308.3	332.4	262.6
rms	kHz	4.6	2.8	1.5	2.9

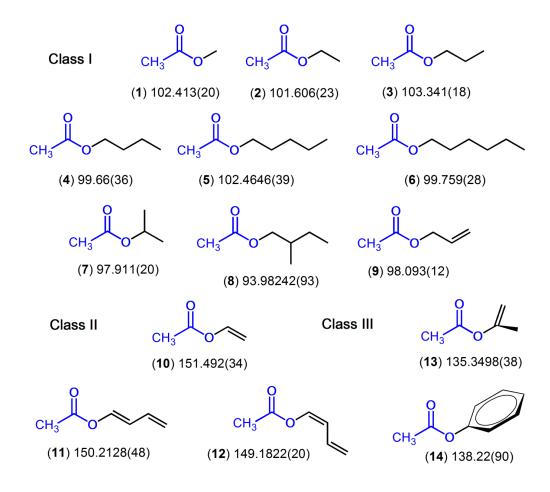# Variety of large amplitude motions in molecules and their applications

This section gives an overview of different molecular classes, each of which features an invididual character on LAMs. The information deduced from the interpretation of the microwave spectra is discussed, mainly the barrier heights but also their applications on structure determinations.

1. Challenges in internal rotation problems: *Some examples*

1.1. Torsional barriers in acetates: *Low (100 to 150 cm⁻¹) and predictable*

The barriers to internal rotation of the acetyl methyl group in acetates (acetic acid esters), **CH₃-COO-R**, have been thoroughly studied. Almost all acetates studied sofar can be divided into three classes, as illustrated in Figure 9. Class I encloses *α,β-saturated acetates*, where the barrier to internal rotation is usually around **100 cm⁻¹**. Examples are *n*-alkyl acetate from methyl acetate [131] up to *n*-hexyl acetate [175,197-200]. Even in the case of isopropyl acetate [201] and isoamyl acetate [202] where the alkyl chain is branched as, or when a double bond is present at the end of the alkyl chain as in allyl acetate [42], the barrier height seems to be almost unaffected.

Class II comprises *α,β-unsaturated acetates* where the C=C double bond is located in the COO plane. The torsional barrier increses from 100 cm⁻¹ to **150 cm⁻¹** due to extended conjugation over the C=C bond. Vinyl acetate [173] and the *E* and the *Z* isomer of butadienyl acetate [203] are two representatives in this class. The two molecules have proven that when the number of conjugated double bonds is augmented, there is no further increase in the barrier height of the acetyl methyl torsion. The configuration of the conjugated double bond system does not influence the barrier significantly, either, since the value of this parameter remains almost the same in the *E* and *Z* isomers of butadienyl acetate [203].

Finally, class III contains *α,β-unsaturated acetates* where the double bond is *not* located in the COO plane. Since the molecule is not planar, the conjugation is less effective than that in the molecules in class II, and the torsional barrier is around **135 cm⁻¹**. Two typical examples of class III are isopropenyl acetate [139] and phenyl acetate [204].
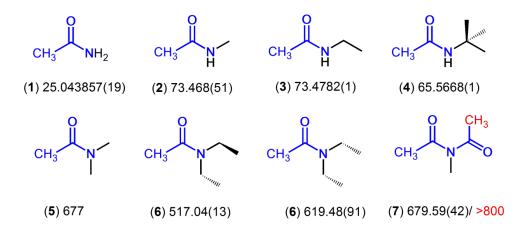

Figure 9. Torsional barriers of the acetyl methyl group in acetates (in cm⁻¹). **Class I:** (**1**) Methyl acetate [131], (**2**) ethyl acetate [175], (**3**) *n*-propyl acetate [197], (**4**) *n*-butyl acetate [198], (**5**) *n*-pentyl acetate [199], (**6**) *n*-hexyl acetate [200], (**7**) isopropyl acetate [201], (**8**) isoamyl acetate [202], and (**9**) allyl acetate [42]. **Class II:** (**10**) Vinyl acetate [173], (**11**) *E* butadienyl acetate [203], and (**12**) *Z* butadienyl acetate [203]. **Class III:** (**13**) Isopropenyl acetate [139] and (**14**) preliminary results of phenyl acetate [204].

1.2. Torsional barriers in acetamides: *Unpredictable.*

The barrier to internal rotation of a methyl group varies strongly, but generally could be devided in three classes. Molecules with torsional barriers higher than 600 cm^{-1} belong to the first class with ethane as the classical example (~1000 cm^{-1}) [205]. The second class comprises of molecules with intermediate barrier heights from about 200 to 600 cm^{-1}. A vast number of one or two-top molecules like *o*-methylanisole [83], 2,5-dimethylfuran [143], and methyl methacrylate [206] fall in this class. Splittings arising from the internal rotation(s) are typically up to some hundreds of MHz. In most cases, taking into account the V_3 term and the internal rotor position is sufficient to model the rotational spectrum with high accuracy. Finally, the last class contains molecules where the methyl group(s) undergo(es) internal rotation(s) with barrier heights lower than 200 cm^{-1}, with a sub-class of very low barriers (say < 30 cm^{-1}). The torsional splittings can be in the order of several GHz, making the assignment of the rotational spectra challenging. In many cases, high order terms are required in the Hamiltonian to model the spectra to experimental accuracy. In the previous section on acetates, a classification can be reliably predicted (see Figure 9). This is not yet the case of acetamides, where a summary is given in Figure 10.

We now focus on the the acetyl methyl group in Figure 10. The acetyl methyl group in acetamide has a remarkably low barrier of 25 cm^{-1} [207]. Probably, the electronic configuration from the amide bond with two hydrogen atoms attached to the nitrogen atom influences the V_3 potential of the methyl group on the other side of the carbonyl group. If one of these hydrogen atoms are substituted, secondary acetamides are obtained, where the barrier is higher than the value found for acetamide, but still low, and varies between 65 and 75 cm^{-1}, depending on the type of the substituent. While the acetyl methyl group in *N-tert*-butylacetamide has a barrier to internal rotation of approximately 65.6 cm^{-1} [184], the respective values of *N*-methylacetamide [195] and *N*-ethylacetamide [174] are both about 73.5 cm^{-1}. Currently, there is no conclusive explaination for this difference.

It is quite impressive that the substitution of one hydrogen atom leads to a difference of approximately 50 cm^{-1} in barrier height between acetamide and the secondary acetamides. If both hydrogen atoms in acetamide are substituted, the effect is

even greater as the barrier height increases by an order of magnitude. For all *tert*-acetamides, the barriers are high, in the order of 500 – 800 cm^{-1} [91,147,208]. Because the substituents are well-separated from the acetyl methyl group by the amide moiety (C=O)N, the reason is probably electronic rather than steric effects. Obviously, the electronic situation is quite special in amides, where information on the electron density can be transferred more easily through the amide bond to the acetyl methyl rotor.

Figure 10. Torsional barriers of the acetyl methyl group in acetamides (in cm^{-1}). (**1**) Acetamide [207], (**2**) *N*-methylacetamide [195], (**3**) *N*-ethylacetamide [174], (**4**) *N-tert*-butylacetamide [184], (**5**) *N,N*-dimethylacetamide [147], (**6**) two conformers of *N,N*-diethylacetamide [91], and (**7**) *N*-methyldiacetamide [208].

1.3. Essentially free internal rotation of the propynyl methyl group: *Very low (< 10 cm^{-1}), very challenging*

Many torsional barriers were accurately determined by using microwave spectroscopy, but only a few studies concern molecules where the barriers are lower than 30 cm^{-1}. Acetamide, mentioned previously in Section 1.2, represents a typical example where the barrier height of the threefold potential is 25 cm^{-1} [207]. Surprisingly, the number of very low barrier investigations does not increase much in the modern ages of microwave spectroscopy. Probably, the reason is the challenge in assigning and fitting roational spectra of molecules with very low torsional barriers, which are in addition hard to
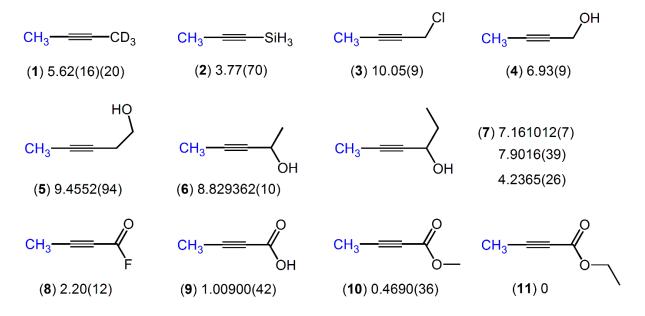
calculate by quantum chemistry. As a consequence of the small number of available studies, the barrier heights cannot be predicted by chemical intuition, either. In some cases such as *trans*-methyl nitrite [209] or *m*-fluorotoluene [210], the comparable values of the threefold- and sixfold potential terms complicated the spectral analysis.

The torsional barriers of the two methyl groups in ethane is high, at around 1000 cm^{-1} [205]. But if a C≡C-triple bond is inserted as a spacer to separate the methyl groups, as in 2-butyne (dimethylacetylene), CH_3−C≡C−CH_3, it is assumed that the molecule exhibits two essentially free methyl internal rotations [211]. Though dimethylacetylene cannot be investigated by microwave spectroscopy due to the lack of a permanent dipole moment, the basic concepts of this chemical bonding suggest that a methyl group connected to an acetylene fragment **CH_3−C≡C−R** (called the propynyl methyl group) features an extremely low torsional barrier ($V_3 < 10$ cm^{-1}). This assumption was confirmed by dimethylacetylene-d_3 (molecule (**1**) in Figure 11) [212] and methylsilylacetylene (**2**) [213], two molecules related to dimethylacetylene possessing a barrier to methyl internal rotation of 5.62(16) and 3.77(70) cm^{-1}, respectively. Very low V_3 potentials of 1.00900(42) and 2.20(12) cm^{-1} were observed for 2-butynoic acid (**9**) (when R = COOH) [214] and tetrolyl fluoride (**8**) (R = COF) [215], respectively.

The torsional barrier of the propynyl methyl group increases to 6.93(9) cm^{-1} in 2-butynol (**4**) (R = CH_2OH) [216]. Currently, the largest value for this group was observed in 1-chloro-2-butyne (**3**) [217] (R = CH_2Cl), for which Solwijk and van Eijck reported a V_3 potential of 10.05(9) cm^{-1}. Three further alkynols, 3-pentyn-1-ol (**5**) [172], 3-pentyn-2-ol (**6**) [218], and 4-hexyn-3-ol (**7**) [219], were studied to find out the effects of the alkyl length on the torsional barrier of the propynyl methyl group. From the results summarized in Figure 11, we found a trend that ***the barrier height decreases slightly by longer alkyl chain***. The barrier height of 2-butynol (**4**) [216] does not fit in this trend, but the authors have reported about a lot of fitting difficulties. Therefore, the barrier of 6.93(9) cm^{-1} might not be as exact as the barriers observed for 3-pentyn-1-ol (**5**), 3-pentyn-2-ol (**6**), and 4-hexyn-3-ol (**7**).

The microwave spectrum of 2-butynoic acid has given the lowest barrier height ever analyzed with a rho axis method Hamiltonian (1.00900(42) cm^{-1}) [214]. The questions

are: Is it still possible to lower this barrier? Can we deduce how structural changes affect the methyl torsional barrier? From the study on the alkynols mentioned aboved, where a decreasing trend by longer alkyl chain was observed, two molecules were investigated where the COOH group in 2-butynoic acid was lengthened to a methoxylate (COO−CH₃) (**10**) and an ethoxylate group (COO−CH₂−CH₃) (**11**). The barrier of 0.4690(36) cm⁻¹ found in methyl-2-butyonate (**10**) [218] provides a new record in low V_3 potential, proving that the methyl group is a good sensor of the molecular structure. For the two conformers of ethyl-2-butyonate (**11**), the internal rotation of the propynyl methyl group is quasi free. A V_3 potential could not be fitted and therefore was fixed to zero in fits with root-mean-square deviation within the measurement accuracy [218].

Figure 11. Torsional barriers of the propynyl methyl group (in cm⁻¹). (**1**) Dimethylacetylene-d_3 [212], (**2**) methylsilylacetylene [213], (**3**) 1-chloro-2-butyne [217], (**4**) 2-butynol [216], (**5**) 3-pentyn-1-ol [172], (**6**) 3-pentyn-2-ol [218], (**7**) 4-hexyn-3-ol [219], (**8**) tetrolyl fluoride [215], (**9**) 2-butynoic acid [214], (**10**) methyl-2-butyonate [218], and (**11**) ethyl-2-butyonate [218].

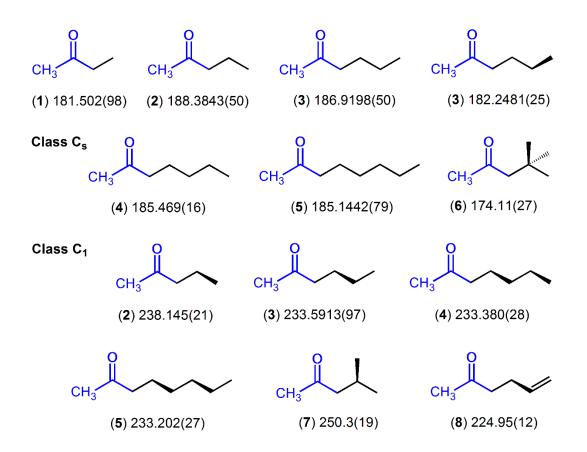## 2. Sensing the molecular conformations of natural substances by internal rotors

2.1. Acetyl methyl torsion in honey bee pheromones: Is the barrier height 180 or 230 cm^{-1}?

Previous sections have shown that the barriers to methyl internal rotation can be linked to functional groups and other structural characteristics of the molecules, making the methyl group a spectroscopic "detector" of the structure. This is quite important if we want to understand eventually the structure and intrinsic properties of larger and more complicated molecules, such as those present in natural substances produced by the plants or biomolecules.

A series of saturated methyl alkyl ketones, naturally present in the honey bee pheromone cocktail, was investigated, starting from ethyl methyl ketone (butan-2-one) to octan-2-one. Except for ethyl methyl ketone, at least two conformers are present in the microwave spectra. One of the two features a C$_s$ structure, where all heavy atomes are located on a symmetry plane, and the other one(s) exhibit(s) C$_1$ symmetry, where the γ-carbon atom of the alkyl chain is bent in a nearly synclinal position. While different conformations possess almost the same barrier height in the cases of *n*-alkyl acetates and methyl alkynoates, this is not the situation found for methyl alkyl ketones where a scheme with two different classes can be drawn, as summarized in Figure 12.

The first class comprises of ketones with a *C$_s$ structure* where the barrier height is always around 180 cm^{-1}. Examples are ethyl methyl ketone [133], the C$_s$ conformer of pentan-2-one [220], hexan-2-one [221], heptan-2-one [222], and octan-2-one. Even, if the alkyl chain is branched, as in the case of methyl neopentyl ketone, the barrier height seems to be almost unaffected [223].

The second class contains molecules with *C$_1$ symmetry* and a higher torsional barrier of approximately 240 cm^{-1}. The C$_1$ conformer of pentan-2-one [220], heptan-2-one [222], octan-2-one, two C$_1$ conformers of hexan-2-one [221], allyl acetone [224] and methyl isobutyl ketone [193] belong to this class. Within each class, the same trend as found for propynyl group containing molecules (Section 1.3.) also applies, i.e. a slightly decrease of the barrier height by longer alkyl chain. This trend is more pronounced in the C$_s$ than in the C$_1$ series (see Figure 12).
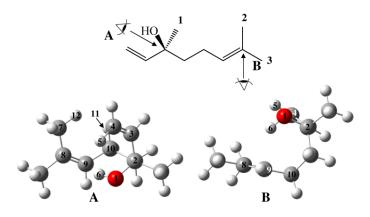
Figure 12. Torsional barriers of the acetyl methyl group in methyl alkyl ketones (in cm^{-1}). (**1**) Ethyl methyl ketone [133], (**2**) pentan-2-one [220], (**3**) hexan-2-one [221], (**4**) heptan-2-one [222], (**5**) octan-2-one (preliminary results), (**6**) methyl neopentyl ketone [223], (**7**) methyl isobutyl ketone [193], and allyl acetone [224].
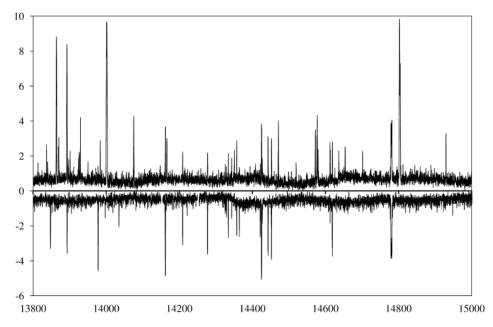
2.2. Conformational determination by internal rotor in lavender oil

Linalool, illustrated in Figure 13, is an acyclic monoterpene. With its agreeable, floral, and refreshing scent, linalool is an important component in several essential oils of plants e.g. lavender (40%), coriander (70%), and ho-leaf (80%). The large size and open chain of linalool offer a rich conformational landscape with hundreds of possible conformers [225]. Among them, finally only one is observed in the jet-cooled microwave spectrum, which is shown in the lower trace of Figure 14. Compared to the spectrum in the same spectral range of the natural product "essence de lavendin", purchased in the Provence, France, (see the upper trace of Figure 14), almost all lines of the linalool spectrum are present with very similar intensity in the spectrum of lavender oil. This shows that high resolution

spectroscopy can be applied to study the chemical compounds used in olfaction as an analytic tool, and to determine the compounds that play an important role for the scent of a perfume.

Figure 13. The globular geometry of the lowest energy conformer of linalool in two different views (A and B) corresponding to the respective Newman projections given in the upper trace. The three methyl groups are labelled with numbers; two of them show resolvable torsional splittings in the experimental spectrum.

Figure 14. Upper trace: the spectrum of essence de lavendin (lavender oil). Lower trace: the linalool spectrum. The frequencies are in MHz; intensities are given in a logarithmic scale and in arbitrary units.

A standard opinion is that a comparison of the experimental rotational constants and those calculated by quantum chemistry is sufficient to validate the molecular structure.

Nevertheless, in the case of linalool, due to the large number of conformers with low energy, the calculated rotational constants of three conformers close in energy are very similar. All of them are in good agreement with the experimentally deduced constants. In order to identify the observed conformer, the angles between the methyl internal rotor axis and the principal axes provided decisive information since those of only one conformer (that given in Figure 13) agree with the experimental ones. Therefore, the internal rotation analysis is crucial for structure determinations in large molecules.

3. Coupled internal rotations

Coupled internal rotations are reported much more rarely. The present section will give an example on a systematic investigation of six isomers of dimethylanisole given in Figure 15 [204].

3.1. From no trouble...

The only member in the family which does not cause fitting troubles is 3,4-dimethylanisole (molecule (**5**) in Figure 15) [128]. It is also the only isomer which exists as two conformers in the microwave spectrum, called *syn* and *anti*, with different orientations of the methoxy group. The torsional barrier of the methyl group in the methoxy moiety -OCH$_3$ (called the methoxy methyl group) is so high, that its internal rotation splittings are not observable with the resolution of the experimental setup. This is in agreement with the study on anisole, which can be treated as a rigid rotor [226]. The coupled LAMs in 3,4-dimethylanisole is therefore a two-top problem, where the methyl groups at the meta- and para-position relative to the methoxy group are the two internal rotors. Because they are located in close proximity, steric hindrance causes an intermediate barrier between 400 and 550 cm^{-1} for both methyl tops which can be modeled well without any top-top coupling term in the Hamiltonian.

Figure 15. Torsional barriers of the methyl groups in six isomers of dimethylanisole (in cm^{-1}). (**1**) 2,3-Dimethylanisole [136], (**2**) 2,4-dimethylanisole [137], (**3**) 2,5-dimethylanisole [204], (**4**) 2,6-dimethylanisole [204], (**5**) 3,4-dimethylanisole [128], and (**6**) 3,4-dimethylanisole [204]. For each compound, "*o*", "*m*", or "*p*" corresponds to the barrier height of the methyl group in the ortho-, meta-, or para-position relative to the –OCH$_3$ methoxy group, respectively. "–OCH$_3$" corresponds to the barrier height of the methoxy methyl group, which is only determinable in 2,6-dimethylanisole (**4**).

3.2. … to some troubles

Two other isomers, 2,4- (**2**) [137] and 2,5-dimethylanisole (**3**) [204], feature an intermediate and a low barrier height. Also in these cases, splittings from the internal rotation of the methoxy methyl group are not observable. The immediate V_3 potential of about 450 cm^{-1} found for the *o*-methyl group is similar in both molecules and probably

also arises from steric hindrance from the neighboghring methoxy group. The methyl rotor at the *para* or *meta* position of 2,4- or 2,5-dimethylanisole, respectively, possesses much lower barrier heights of less than 70 cm^{-1} (see Figure 15) and is thus challenging for the fitting process. The top-top coupling term multiplying $(1 - \cos\alpha_1)(1 - \cos\alpha_2)$ and higher order effective parameters are required in the Hamiltonian to achieve standard deviation close to measurement accuracy [137,204]. The spectral assignments are quite extensive, because every frequency has to be verified by combination difference loops to assure a correct assignment.

3.3. … and a lot of troubles

Since the 3,4-isomer is a "no-trouble-case" due to steric hindrance of the two neighboring methyl groups, which increases the barrier heights to intermediate values, one tends to assume that 2,3-dimethylanisole (**1**), also featuring two neighboring methyl groups, would not cause any fitting troubles, either. This assumption finally turns out to be wrong. In 2,3-dimethylanisole (**1**), while the V_3 potential of 519 cm^{-1} of the *m*-methyl group is intermediate can be treated well, the surprisingly low barrier to internal rotation of about 27 cm^{-1} of the methyl group at the *ortho* position cannot be captured correctly with the *XIAM* program [136]. Assuming that a methoxy group and a methyl group are similar, then the *o*-methyl group, featuring a C$_{3v}$ symmetry, would experience potentials on a frame with C$_{2v}$ symmetry, similar to the cases of toluene [22] or nitromethane [182], where the V_3 contribution of the potential vanishes and only a small V_6 term exists. In the case of 2,3-dimethylanisole, the frame symmetry is out-of-balance from C$_{2v}$, resulting in a small V_3 term of about 27 cm^{-1}. This very low V_3 potential term is challenging for the spectral analysis. The situation gets even worse in the case of 3,5-dimethylanisole (**6**), where both ring methyl groups undergo internal rotation with low torsional barriers [204].

3.4. But also some nice surprise: *Lowering the torsional barrier by sterical hindrance*

Sterical hindrance is known to increase the barrier to methyl internal rotation, because the methyl torsion is not only hindered quantum mechanically, but also

mechanically if a bulky group is present in close proximity of the methyl group. However, there are exceptions.

In all five isomers of dimethylanisole mentioned previously, slittings due to the internal rotation of the methoxy methyl group have never been observed. This is in agreement with the experimental results of anisole, as well as the high torsional barriers of over 1000 cm^{-1} predicted by quantum chemistry. All these isomers have a common structural feature: the methoxy group is always located on the phenyl ring plane, which is at the same time the symmetry plane.

The situation changes in 2,6-dimethylanisole (**4**): Because of steric hindrance caused by the two methyl groups occupying both ortho-positions of the phenyl ring, the methoxy group located between them is forced to tilt out of the phenyl plane by 90°. The molecular symmetry is still C$_s$, but the symmetry plane is now perpendicular to the plane containing the phenyl ring, and the two ring methyl groups are equivalent [204] (see Figure 15). This extraordinary orientation of the methoxy methyl group in 2,6-dimethylanisole has decreased its torsional barrier height from over 1000 cm^{-1} to 457 cm^{-1}, and torsional splittings become resolvable. Therefore, this isomer surprisingly presents a three-top problem with totally 10 torsional species. The potential barriers of the two equivalent methyl groups are approximately 200 cm^{-1} [204].
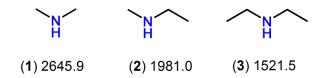
4. Inversion tunneling

As mentioned in the section on Large Amplitude Motions, much less investigations have been reported on inversion tunneling motions than on internal rotations. In addition, inversion tunneling is often combnied with internal rotation. Only in very few molecules like *planar secondary amines*, the inversion tunneling of the proton at the nitrogen atom is not accompanied by internal rotation. This section will focus on a series of such molecules, starting from dimethyl amine [158], then ethyl methyl amine [159], and diethyl amine [160].

The *c*-component of the dipole moment changes sign, while the *b*-component retains its sign during the proton inversion (see Figure 16). Therefore, tunneling splittings are observed in the spectrum for all *c*-type transitions, which are twice the separation between the lowest symmetric and anti-symmetric inversion energy levels. The values of these splittings are given in Figure 17. A trend can be easily recognized that the splittings decrease in larger molecules.
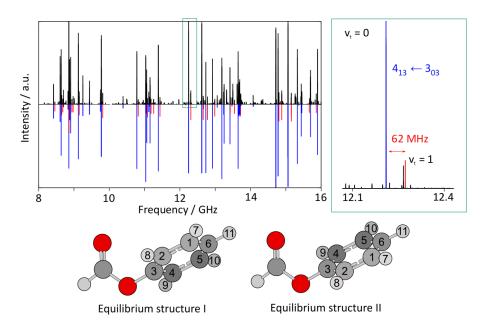

Figure 16. The potential energy curve describing the inversion tunneling at the nitrogen atom of diethyl amine. The angle θ is the angle of the NH bond against the NCC plane. Inset: Horizontal lines indicate the lowest torsional energy levels $v_t = 0, 1, 2, 3$, which are doubly degenerated. The two versions of the equilibrium geometry given in the lower trace correspond to the two energy minima of the nitrogen tunneling process. The two equilibrium structures on the lower figure show that the dipole moment, indicated as a red arrow, changes sign in the *c*-direction upon proton tunneling.

(**1**) 2645.9   (**2**) 1981.0   (**3**) 1521.5

Figure 17. Tunneling splittings of *c*-type transitions in secondary amines (in MHz). (**1**) Dimethyl amine [158], (**2**) ethyl methyl amine [159], and (**3**) diethyl amine [160].

Phenyl formate also features a pure inversion tunneling motion, which is the tunneling of the phenyl ring [227]. At the beginning, phenyl formate was expected as a normal rigid-rotor molecule, but a rigid-rotor model has failed completely to reproduce its microwave spectra with a root-mean-square deviation of 3 MHz while the measurement accuracy was 2 kHz. Quantum chemical calculations have hinted that some state other than the ground state is populated in the molecular jet, as a consequence of the ring tunneling quantum effect. This low-lying $v_t = 1$ tunneling state is calculated to lie at 48.24 GHz (1.6 cm^{-1}) above the $v_t = 0$ ground state, corresponding to tunneling splittings in the order of about 100 GHz for all *c*-type transitions. For a comparision, the largest splittings observed for the secondary amines illustrated in Figure 18 are 2.6459 GHz, found in dimethyl amine [158]. The splittings arising for *b*-type transitions due to Coriolis interaction are up to 100 MHz, three order of magnitude larger than those found in the the secondary amines, as depicted in Figure 18.

Figure 18. *Upper figure, left hand side*: A portion from 8 to 16 GHz of the survey spectrum of phenyl formate (upper trace) compared to the theoretical spectrum (lower trace) predicted using the program *SPFIT/SPCAT*. Transitions of the $v_t = 0$ ground state are marked in blue, those of the $v_t = 1$ excited state in red. *Right hand side*: The frequency range from 12.1 to 12.4 GHz in an enlarged scale, capturing the $v_t = 0$ and $v_t = 1$ components of the $4_{13} \leftarrow 3_{03}$ transition which are separated by 62 MHz due to Coriolis interactions. *Lower figure*: Two versions of the equilibrium geometry corresponding to the two energy minima of the ring tunneling process.

Conclusion

A large variety of molecular systems with applications in diverse research fields, from molecular biology, astrophysics, to environmental sciences contain large amplitude motions. Studying them at the molecular level is an extremely lively field. The focus of the present review was on two types of large amplitude motions which frequently occur: internal rotation and inversion tunneling. The combination of molecular jet Fourier transform microwave spectroscopy, spectral modeling, and quantum chemical calculations is particularly successful in decoding complex spectra with large amplitude motions and providing reference data for astrophysical research, atmospheric chemistry, or general applications in physical chemistry.

The two most popular types of state-of-the-art Fourier transform microwave spectrometer technology based on pulsed supersonic jet expansions are resonator-based and chirped-pulse spectrometers. The former version is commonly used in many microwave laboratories and has shown its superior sensitivity and resolving power, but suffers from the time requirement to acquire survey spectra, because the resonator has to be tuned mechanically for every frequency element at rather narrow steps of less than 0.25 MHz. The later version relies on a very short but powerful frequency-ramp signal with a band width of 1 GHz and thus provides unparalleled speed for scans with more reliable line intensities.

The use of quantum chemistry using programs such as *Gaussian* or *GAMESS* as a supporting tool for rotational spectroscopy is becoming very popular. The most common methods used by many microwave spectroscopic labs is the density functional theory using the B3LYP functional and the MP2 method, along with the Pople valence triple-zeta basis set 6-311++G(d,p). Conformational analysis performed by calculating potential energy surfaces and geometry optimizations are sufficiently accurate to start the spectral assignment. In the contrary, predicting the barriers of large amplitude motions,

corresponding to calculations of energy, is not yet sufficiently accurate to satisfy experimental requirements and needs experimental values for benchmark calculations.

Several computer codes for global fits of rotational spectra with splittings arising from large amplitude motions have been developed along the last four or five decades, among them, not exhautively *SPFIT/SPCAT, IAMCALC, JB95, XIAM, BELGI, RAM36, PAM-C$_{2v}$-2tops*, and *Erham*, just to mention some of them. A local approach such as in the *SFLAMS* code for separately fitting the large amplitude motion species can ease the assignments of the microwave spectra, especially when a large number of internal rotors (> 3) and low torsional barriers have to be conquered and it is still challenging to model the splittings in a global approach. Some "problematic", yet unsolved cases remain where the internal rotation(s) interact(s) with tunneling motion(s) or with other small amplitude vibrations. Theoretical developments and new codes are needed for those cases.

Some examples on chemical aspects and comparison of barrier heights in systematic investigations on acetates, amides, propynyl group containing molecules, ketones, and dimethylanisoles as well as the inversion tunneling in secondary amines and phenyl formate have given information about how large amplitude motions can help us to understand molecular structures and conformations in nature. Applications of large amplitude motions on conformational determinations are only at their beginning on natural substances and biomolecules where they can provide unique "sensors" of the molecular structure. There is no doubt that many future investigations towards this direction with great potential will be performed.

References

[1] T. J. Balle, E. J. Campbell, M. R. Keenan, W. H. Flygare, J. Chem. Phys. **71**, 2723 (1979).

[2] T. J. Balle and W. H. Flygare, Rev. Sci. Instrum. **52**, 33 (1981).

[3] C. H. Townes and A. L. Schawlow, ''Microwave Spectroscopy'', McGraw-Hill, New York, 1955.

[4] W. Gordy and L. R. Cook, ''Microwave Molecular Spectra'', 3rd Edition, in Weissberger, A. (ED.), Techniques of Chemistry, vol. XVIII, John Wiley & Sons Inc., New York, 1984.

[5] J. E. Wollrab, ''Rotational Spectra and Molecular Structure'', Academic press, New York, 1967.

[6] D. G. Lister, J. N. Macdonald, N. L. Owen, ''Internal Rotation and Inversion: An Introduction to Large Amplitude Motions in Molecules'', Academic Press, New York, 1978.

[7] C. C. Lin and J. D. Swalen, *Rev. Mod. Phys.* **31**, 841 (1959).

[8] P. R. Bunker and P. Jensen, ''Molecular Symmetry and Spectroscopy'', NRC Research Press, Ottawa, 1998.

[9] H. M. Pickett, *J. Mol. Spectrosc.* **148**, 371 (1991).

[10] H. M. Pickett, R. L. Poynter, E. A. Cohen, M. L. Delitsky, J. C. Pearson, H. S. P. Müller, *J. Quant. Spectrosc. Rad. Transfer* **60**, 883 (1998). – See also SPFIT/SPCAT package at the Jet Propulsion Laboratory (JPL), http://spec.jpl.nasa.gov.

[11] C. P. Endres, S. Schlemmer, P. Schilke, J. Stutzki, H. S. P. Müller, The Cologne Database for Molecular Spectroscopy, CDMS, in the Virtual Atomic and Molecular Data Centre, VAMDC. *J. Mol. Spectrosc.* **327**, 95 (2016). – See also the Cologne Database for Molecular Spectroscopy (CDMS) website, https://cdms.astro.uni-koeln.de/.

[12] A. J. Markwick-Kemper, A. J. Remijan, "The Splatalogue (Spectral Line Catalogue) and Calibase (Calibration Source Database)", *Bull. Am. Astron. Soc.* **38**, 130 (2006). – See also: Splatalogue: database for astronomical spectroscopy website, https://www.cv.nrao.edu/php/splat/

[13] F. J. Lovas (2009), NIST Recommended Rest Frequencies for Observed Interstellar Molecular Microwave Transitions, DOI: https://dx.doi.org/10.18434/T4JP4Q

[14] Toyama Microwave Atlas for spectroscopists and astronomers, 2017, http://www.sci.u-toyama.ac.jp/phys/4ken/atlas/

[15] http://info.ifpan.edu.pl/~kisiel/prospe.htm

[16] H. Hartwig and H. Dreizler, *Z. Naturforsch.* **51a**, 923 (1996).

[17] N. Ohashi and J. T. Hougen, *J. Mol. Spectrosc.* **203**, 170 (2000).

[18] J. T. Hougen, I. Kleiner, M. Godefroid, *J. Mol. Spectrosc.* **163**, 559 (1994).

[19] I. Kleiner and J. T. Hougen, *J. Chem. Phys.* **119**, 5505 (2003).

[20] M. Tudorie, I. Kleiner, J. T. Hougen, S. Melandri, L. W. Sutikdja, W. Stahl, *J. Mol. Spectrosc.* **269**, 211 (2011).

[21] P. Groner, *J. Chem. Phys.* **107**, 4483 (1997).

[22] V. V. Ilyushin, Z. Kisiel, L. Pszczółkowski, H. Mäder, J. T. Hougen, *J. Mol. Spectrosc.* **259**, 26 (2010).

[23] V. V. Ilyushin and J. T. Hougen, *J. Mol. Spectrosc.* **289**, 41 (2013).

[24] D. F. Plusquellic, R. D. Suenram, B. Mate, J. O. Jensen, A. C. Samuels, *J. Chem. Phys.* **115**, 3057 (2001).

[25] I. Kleiner, J. T. Hougen, *J. Phys. Chem. A* **119**, 10664 (2015).

[26] M. J. Frisch, G. W. Trucks, H. B. Schlegel, G. E. Scuseria, M. A. Robb, J. R. Cheeseman, G. Scalmani, V. Barone, G. A. Petersson, H. Nakatsuji, X. Li, M. Caricato, A. V. Marenich, J. Bloino, B. G. Janesko, R. Gomperts, B. Mennucci, H. P. Hratchian, J. V. Ortiz, A. F. Izmaylov, J. L. Sonnenberg, D. Williams-Young, F. Ding, F. Lipparini, F. Egidi, J. Goings, B. Peng, A. Petrone, T. Henderson, D. Ranasinghe, V. G. Zakrzewski, J. Gao, N. Rega, G. Zheng, W. Liang, M. Hada, M. Ehara, K. Toyota, R. Fukuda, J. Hasegawa, M. Ishida, T. Nakajima, Y. Honda, O. Kitao, H. Nakai, T. Vreven, K. Throssell, J.A. Montgomery, Jr., J. E. Peralta, F. Ogliaro, M. J. Bearpark, J. J. Heyd, E. N. Brothers, K. N. Kudin, V. N. Staroverov, T. A. Keith, R. Kobayashi, J. Normand, K. Raghavachari, A. P. Rendell, J. C. Burant, S. S. Iyengar, J. Tomasi, M. Cossi, J. M. Millam, M. Klene, C. Adamo, R. Cammi, J. W. Ochterski, R. L. Martin, K. Morokuma, O. Farkas, J. B. Foresman, D. J. Fox, Gaussian 16, Revision B.01, Inc., Wallingford CT, 2016.

[27] M. W. Schmidt, K. K. Baldridge, J. A. Boatz, S. T. Elbert, M. S. Gordon, J. J. Jensen, S. Koseki, N. Matsunaga, K. A. Nguyen, S. Su, T. L. Windus, M. Dupuis, J. A. Montgomery, *J. Comput. Chem.* **14**, 1347 (1993).

[28] J.-U. Grabow, Fourier Transform Microwave Spectroscopy Measurement and Instrumentation. In Handbook of High-Resolution Spectroscopy; M. Quack, F. Merkt, Eds.; Wiley: Chichester, U.K., 2011; Vol. 2, Chapter 1.

[29] J.-U. Grabow, E. S. Palmer, M. C. McCarthy, P. Thaddeus, *Rev. Sci. Instrum.* **76**, 093106 (2005).

[30] J. L. Alonso, C. Pérez, M. E. Sanz, J. C. López, S. Blanco, *Phys. Chem. Chem. Phys.* **11**, 617 (2009).

[31] E. J. Cocinero, A. Lesarri, P. Écija, J.-U. Grabow, J. A. Fernández, F. Castaño, *Phys. Chem. Chem. Phys.* 12, 12486 (2010).

[32] J.-U. Grabow, Habilitationschrift, Hannover University (1994).

[33] J.-U. Grabow, W. Stahl, H. Dreizler, *Rev. Sci. Instrum.* **67**, 4072 (1996).

[34] J. R. Avilés Moreno, J. Demaison, T. R. Huet, *J. Am. Chem. Soc.* **128**, 10467 (2006).

[35] Y. Xu, W. Jäger, *J. Chem. Phys.* **106**, 7968 (1997).

[36] G. Sedo, J. van Wijngaarden, *J. Chem. Phys.* **131**, 044303 (2009).

[37] H. O. Leung, D. Gangwani, J.-U. Grabow, *J. Mol.Spectrosc.* **184**, 106 (1997).

[38] R. C. Batten, G. C. Cole, A. C. Legon, *J. Chem. Phys.* **119**, 7903 (2003).

[39] A. R. Hight Walker, W. Chen, S. E. Novick, B. D. Bean, M. D. Marshall, *J. Chem. Phys.* **102**, 7298 (1995).

[40] J. J. Newby, M. M. Serafin, R. A. Peebles, S. A. Peebles, *Phys. Chem. Chem. Phys.* **7**, 487 (2005).

[41] I. Merke, W. Stahl, H. Dreizler, *Z. Naturforsch.* **49a**, 490 (1994).

[42] H. V. L. Nguyen, H. Mouhib, W. Stahl, I. Kleiner, *Mol. Phys.* **108**, 763 (2010).

[43] J. J. Pajski, M. D. Logan, K. O. Douglass, G. G. Brown, R. D. Suenram, B. C. Dian, B. H. Pate, *Int. J. high speed electron.* **18**, 31 (2008).

[44] D. Loru, M. A. Bermúdez, M. E. Sanz, *J. Chem. Phys.* **145**, 074311 (2016).

[45] D. Schmitz, V. A. Shubert, T. Betz, M. Schnell, *J. Mol. Spectrosc.* **280**, 77 (2012).

[46] J. L. Neill, S. T. Shipman, L. Alvarez-Valtierra, A. Lesarri, Z. Kisiel, B. H. Pate, *J. Mol. Spectrosc.* **269**, 21 (2011).

[47] F. E. Marshall, D. J. Gillcrist, T. D. Persinger, S. Jaeger, C. C. Hurley, N. E. Shreve, N. Moon, G. S. Grubbs II, *J. Mol. Spectrosc.* **328**, 59 (2016).

[48] A. O. Hernandez-Castillo, C. Abeysekera, B. M. Hays, T. S. Zwier, *J. Chem. Phys.* **145**, 114203 (2016).

[49] I. A. Finneran, D. B. Holland, P. B. Carroll, G. A. Blake, *Rev. Sci. Instrum.* **84**, 083104 (2013).

[50] K. N. Crabtree, M. A. Martin-Drumel, G. G. Brown, S. A. Gaster, T. M. Hall, M. C. McCarthy, *J. Chem. Phys.* **144**, 124201 (2016).

[51] S. Mata, I. Peña, C. Cabezas, J. C. López, J. L. Alonso, *J. Mol. Spectrosc.* **280**, 91 (2012).

[52] I. Uriarte, P. Écija, L. Spada, E. Zabalza, A. Lesarri, F. J. Basterretxea, J. A. Fernández, W. Caminati, E. J. Cocinero, *Phys. Chem. Chem. Phys.* **18**, 3966 (2016).

[53] J.-U. Grabow, S. Mata, J. L. Alonso, I. Peña, S. Blanco, J. C. López, C. Cabezas, *Phys. Chem. Chem. Phys.* **13**, 21063 (2011).

[54] S. P. Dempster, O. Sukhorukov, Q.-Y. Lei, W. Jäger, *J. Chem. Phys.* **137**, 174303 (2012).

[55] L. Evangelisti, G. Sedo, J. van Wijngaarden, *J. Phys. Chem. A* **115**, 685 (2011).

[56] M. D. Marshall, H. O. Leung, B. Q. Scheetz, J. E. Thaler, J. S. Muenter, *J. Mol. Spectrosc.* **266**, 37 (2011).

[57] S. L. Stephens and N. R. Walker, *J. Mol. Spectrosc.* **263**, 27 (2010).

[58] G. S. Grubbs II, C. T. Dewberry, K. C. Etchison, K. E. Kerr, S. A. Cooke, *Rev. Sci. Instrum.* **78**, 096106 (2007).

[59] D. A. Obenchain, A. A. Elliott, A. L. Steber, R. A. Peebles, S. A. Peebles, C. J. Wurrey, G. A. Guirgis, *J. Mol. Spectrosc.* **261**, 35 (2010).

[60] V. Van, W. Stahl, H. V. L. Nguyen, *J. Mol. Struct.* **1123**, 24 (2016).

[61] H.V.L. Nguyen, *J. Mol. Struct.* **1208**, 127909 (2020).

[62] J. B. Graneek, W. C. Bailey, M. Schnell, *Phys. Chem. Chem. Phys.* **20**, 22210 (2018).

[63] H. Mouhib, *J. Phys. B: At. Mol. Opt. Phys.* 47, 143001 (2014).

[64] C. J. Cramer, Essentials of Computational Chemisty—Theories and Models, 2nd edn (Chichester Wiley), 2004.

[65] F. Jensen, Introduction to Computational Chemistry (Chichester, Wiley), 2007.

[66] L. Ferres, W. Stahl, H. V. L. Nguyen, *Mol. Phys.* **114**, 2788 (2016).

[67] A. D. Becke, *J. Chem. Phys.* **98**, 5648 (1993)

[68] C. Lee, W. Yang, R. G. Parr, *Phys. Rev. B* **37**, 785 (1988).

[69] C. Møller and M. S. Plesset, *Phys. Rev.* **46**, 618 (1934).

[70] K.P. Rajappan Nair, S. Herbers, J.-U. Grabow, *J. Mol. Spectrosc.* **355**, 19 (2019).

[71] A. Karpfen, C. H. Choi, M. Kertesz, *J. Phys. Chem. A* **101**, 7426 (1997).

[72] S. Grimme, J. Antony, S. Ehrlich, H. Krieg, *J. Chem. Phys.* **132**, 154104 (2010).

[73] S. Grimme, S. Ehrlich, L. Goerigk, *J. Comput. Chem.* **32**, 1456 (2011).

[74] I. Uriarte, A. Insausti, E. J. Cocinero, A. Jabri, I. Kleiner, H. Mouhib, I. Alkorta, *J. Phys. Chem. Lett.* **9**, 5906 (2018).

[75] H. V. L. Nguyen and W. Stahl, *ChemPhysChem* **12**, 1900 (2011).

[76] R. Krishnan and J. A. Pople, *Int. J. Quant. Chem.* **14**, 91 (1978).

[77] R. J. Bartlett and M. Musial, *Rev. Mod. Phys.* **79**, 291 (2007).

[78] J. A. Pople, M. Head-Gordon, D. J. Fox, K. Raghavachari, L. A. Curtiss, *J. Chem. Phys.* **90**, 5622 (1989).

[79] T. H. Dunning Jr, *J. Chem. Phys.* **90**, 1007 (1986)

[80] H. Mouhib, V. Van, W. Stahl, *J. Phys. Chem. A* **117**, 6652 (2013).

[81] C. Pérez, M. T. Muckle, D. P. Zaleski, N. A. Seifert, B. Temelso, G. C. Shields, Z. Kisiel, B. H. Pate, *Science* **336**, 897 (2012).

[82] V. Van, W. Stahl, M. Schwell, H.V.L. Nguyen, *J. Mol. Struct.* **1156**, 348 (2018).

[83] L. Ferres, H. Mouhib, W. Stahl, H. V. L. Nguyen, *ChemPhysChem* **18**, 1855 (2017).

[84] L. Ferres, W. Stahl, H. V. L. Nguyen, *J. Chem. Phys.* **148**, 124304 (2018).

[85] L. Ferres, W. Stahl, I. Kleiner, H. V. L. Nguyen, *J. Mol. Spectrosc.* **343**, 44 (2018).

[86] H. Mouhib and W. Stahl, *ChemPhysChem* **13**, 1297 (2012).

[87] H.V.L. Nguyen, J.-U. Grabow, *ChemPhysChem* (2020). DOI: 10.1002/cphc.202000234

[88] Z. Kisiel, O. Desyatnyk, L. Pszczółkowski, S. B. Charnley, P. Ehrenfreund, *J. Mol. Spectrosc.* **217**, 115 (2003).

[89] S. Grimme and M. Steinmetz, *Phys. Chem. Chem. Phys.* **15**, 16031 (2013).

[90] J. Demaison, A. G. Császár, L.D. Margulès, H.D. Rudolph, *J. Phys. Chem. A* **115**, 14078 (2011).

[91] R. Kannengießer, S. Klahm, H. V. L. Nguyen, A. Lüchow, W. Stahl, *J. Chem. Phys.* **141**, 204308 (2014).

[92] C. E. Cleeton and N. H. Williams, *Phys. Rev.* **45**, 234 (1934).

[93] R. Meyer, J. C. López, J. L. Alonso, S. Melandri, P. G. Favero, W. Caminati, *J. Chem. Phys.* **111**, 7871 (1999).

[94] J. T. A. Gall, J. Thomas, F. Xie, Z. Wang, W. Jäger, Y. Xu, *Phys. Chem. Chem. Phys.* **19**, 29508 (2017).

[95] J. S. Koehler and D. M. Dennison, *Phys. Rev.* **57**, 1006 (1940).

[96] R. H. Hughes, W. E. Good, D. K. Coles, *Phys. Rev.* **84**, 418 (1951).

[97] R. M. Lees and J. G. Baker, *J. Chem. Phys.* **48**, 5299 (1968).

[98] F. C. De Lucia, E. Herbst, T. Anderson, P. Helminger, *J. Mol. Spectrosc.* **134**, 395 (1989).

[99] L.-H. Xu, J. Fisher, R. M. Lees, H. Y. Shi, J. T. Hougen, J. C. Pearson, B. J. Drouin, G. A. Blake, R. Braakman, *J. Mol. Spectrosc.* **251**, 305 (2008).

[100] C. C. Lin and R. W. Kilb, *J. Chem. Phys.* **24**, 631 (1956).

[101] A. Bauder and H. H. Günthard, *J. Mol. Spectrosc.* **60**, 290 (1976).

[102] W. Liang, J. G. Baker, E. Herbst, R. A. Booker, F. C. De Lucia, *J. Mol. Spectrosc.* **120**, 298 (1986).

[103] H. Maes, G. Wlodarczak, D. Boucher, J. Demaison, *Z. Naturforsch.* **42a**, 97 (1987).

[104] R. F. Curl, *J. Chem. Phys.* **30**, 1529 (1959).

[105] G. M. Plummer, G. A. Blake, E. Herbst, F. C. De Lucia, *Astrophys. J. Suppl.* **55**, 633 (**1984**).

[106] J. Demaison, D. Boucher, A. Dubrulle, B. P. Van Eijck, *J. Mol. Spectrosc.* **102**, 260 (1983).

[107] L. C. Oesterling, S. Albert, F. C. De Lucia, K. V. L. N. Sastry, E. Herbst, *Astrophys. J.* **521**, 255 (1999).

[108] K. Oka, Y. Karakawa, H. Odashima, K. Takagi, S. Tsunekawa, *J. Mol. Spectrosc.* **210**, 196 (2001).

[109] B. P. Van Eijck, J. Van Ophensden, M. M. M. Van Schaik, E. Van Zoeren, *J. Mol. Spectrosc.* **86**, 465 (1981).

[110] Demaison, A. Dubrulle, D. Boucher, J. Burie, B. P. van Eijck, *J. Mol. Spectrosc.* **94**, 211 (1982).

[111] W. J. Tabor, *J. Chem. Phys.* **27**, 974 (1957).

[112] C. C. Krischer, E. Saegebarth, *J. Chem. Phys.* **54**, 4553 (1971).

[113] I. Kleiner, ACS Earth Space Chem. **3,** 1812 (2019).

[114] E. Fischer and I. Botskor, *J. Mol. Spectrosc.* **91**, 116 (1982).

[115] E. Fischer and I. Botskor, *J. Mol. Spectrosc.* **104**, 226 (1984).

[116] M. Canagaratna, J. A. Phillips, M. E. Ott, K. R. Leopold, *J. Phys. Chem. A* **102**, 1489 (1998).

[117] G. Columberg, A. Bauder, N. Heineking, W. Stahl, J. Makarewicz, *Mol. Phys.* **93**, 215 (1998).

[118] F. J. Lovas, D. R. Johnson, D. Buhl, L.E. Snyder, *Astrophys. J.* **209**, 770 (1976).

[119] E. Churchwell and W. G. Winnewisser, *Astron. Astrophys.* **45,** 229 (1975).

[120] M. B. Bell, H. E. Matthews, P. A. Feldman, *Astron. Astrophys.* **127**, 420 (1983).

[121] H. E. Matthews, P. Friberg, W. M. Irvine, *Astron. Astrophys.* **290**, 609 (1985).

[122] D. M. Mehringer, L. E. Snyder, Y. Miao, F. J. Lovas, *Astrophys. J.* **480**, 71 (1997).

[123] C. W. Lee, S. H. Cho, S. M. Lee, *Astrophys. J.* **551**, 333 (2001).

[124] F. Combes, M. Gerin, A. Wootten, G. Wlodarczak, F. Clausset, P. J. Encrenaz, *Astron. Astrophys.* **180**, 13 (1987).

[125] G. W. Fuchs, U. Fuchs, T. F. Giesen, F. Wyrowski, *Astron. Astrophys.* **444**, 521 (2005).

[126] B. Tercero, I. Kleiner, J. Cercicharo, H. V. L. Nguyen, A. López, G. M. Munoz Caro, *Astrophys. J.* **770**, L13 (2013).

[127] H. Dreizler, *Z. Naturforsch.* **16a**, 1354 (1961).

[128] L. Ferres, J. Cheung, W. Stahl, H. V. L. Nguyen, *J. Phys. Chem. A* **123**, 3497 (2019).

[129] V. Van, W. Stahl, H. V. L. Nguyen, *Phys. Chem. Chem. Phys.* **17**, 32111 (2015).

[130] J. Sheridan, W. Bossert, A. Bauder, *J. Mol. Spectrosc.* **80**, 1 (1980).

[131] H. V. L. Nguyen, I. Kleiner, S. T. Shipman, Y. Mae, K. Hirose, S. Hatanaka, K. Kobayashi, *J. Mol. Spectrosc.* **299**, 17 (2014).

[132] V. Van, W. Stahl, H. V. L. Nguyen, *ChemPhysChem* **17**, 3223 (2016).

[133] H. V. L. Nguyen, V. Van, W. Stahl, I. Kleiner, *J. Chem. Phys.* **140**, 214303 (2014).

[134] H. V. L. Nguyen, W. Stahl, I. Kleiner, *Mol. Phys.* **110**, 2035 (2012).

[135] M. Tudorie, I. Kleiner, M. Jahn, J.-U. Grabow, M. Goubet, O. Pirali, *J. Phys. Chem. A.* **117**, 13636 (2013).

[136] L. Ferres, K.-N. Truong, W. Stahl, H. V. L. Nguyen, *ChemPhysChem* **19**, 1781 (2018).

[137] L. Ferres, W. Stahl, H. V. L. Nguyen, *J. Chem. Phys.* **151**, 104310 (2019).

[138] S. Herbers, S. M. Fritz, P. Mishra, H. V. L. Nguyen, T. S. Zwier, *J. Chem. Phys.* **152**, 074301 (2020).

[139] H. V. L. Nguyen and W. Stahl, *J. Mol. Spectrosc.* **264**, 120 (2010).

[140] P. Groner, S. Albert, E. Herbst, F. C. De Lucia, F. J. Lovas, B. J. Drouin, J. C. Pearson, *Astrophys. J.* **142**, 145 (2002).

[141] W. Neustock, A. Guarnieri, J. Demaison, G. Wlodarczak, *Z. Naturforsch.* **45a**, 702, 1990.

[142] P. Groner, C. W. Gillies, J. Z. Gillies, Y. Zhang, E. Block, *J. Mol. Spectrosc.* **226**, 169 (2004)

[143] V. Van, J. Bruckhuisen, W. Stahl, V. Ilyushin, H. V. L. Nguyen, *J. Mol. Spectrosc.* **343**, 121 (2018).

[144] A. Jabri, V. Van, H. V. L. Nguyen, H. Mouhib, F. Kwabia-Tchana, L. Manceron, W. Stahl, I. Kleiner, *Astron. Astrophys.* **589**, A127 (2016).

[145] I. Merke, A. Lüchow, W. Stahl, *J. Mol. Struct.* **780-781**, 295 (2006).

[146] M. Schnell, J. T. Hougen, J.-U. Grabow, *J. Mol. Spectrosc.* **251**, 38 (2008).

[147] M. Fujitake, Y. Kubota, N. Ohashi, *J. Mol. Spectrosc.* **236**, 97 (2006).

[148] K. M. Marstokk and H. Møllendal, *J. Mol. Struct.* **49**, 221 (1978).

[149] I. Merke and L. H. Coudert, *J. Mol. Spectrosc.* **237**, 174 (2006).

[150] T. Kasuja, *Sci. Papers Inst. Phys. Chem. Res. Tokyo* **56**, 1 (1962).

[151] S. Tsunekawa, T. Kojima, J. T. Hougen, *J. Mol. Spectrosc.* **95**, 133 (1982).

[152] M. Kreglewski, J. Cosléou, G. Wlodarczak, *J. Mol. Spectrosc.* **216**, 501 (2002).

[153] I. Gulaczyk, J. Pyka, M. Kręglewsk, *J. Mol. Spectrosc.* **241**, 75 (2007).

[154] I. Gulaczyk and M. Kręglewski, *J. Mol. Spectrosc.* **249**, 73 (2008).

[155] B. Kleibömer and D. H. Sutter, *Z. Naturforsch.* **43a**, 561 (1988).

[156] N. Ohashi and J. T. Hougen, *J. Mol. Spectrosc.* **170**, 493 (1995).

[157] F. J. Lovas, S. P. Belov, M. Y. Tretyakov, W. Stahl, R. D. Suenram, *J. Mol. Spectrosc.* **170**, 478 (1995).

[158] J. E. Wollrab and V. W. Laurie, *J. Chem. Phys.* **48**, 5058 (1968).

[159] R. E. Penn and J. E. Boggs, *J. Mol. Spectrosc.* **47**, 340 (1973).

[160] H. V. L. Nguyen and W. Stahl, *J. Chem. Phys.* **135**, 024310 (2011).

[161] L. Ferres, H. Mouhib, W. Stahl, M. Schwell, H. V. L. Nguyen, *J. Mol. Spectrosc.* **337**, 59 (2017).

[162] I. Gulaczyk and M. Kręglewski, *J. Mol. Spectrosc.* **256**, 86 (2009).

[163] I. Gulaczyk, M. Kręglewski, V-M. Horneman, *J. Mol. Spectrosc.* **270**, 70 (2011).

[164] I. Gulaczyk and M. Kręglewski, *J. Quant. Spectrosc. Radiat. Transf.* **217**, 321 (2018).

[165] S. L. Baughcum, Z. Smith, E. B. Wilson, R. W. Duerst, *J. Am. Chem. Soc.* **106**, 2260 (1984).

[166] Y.-C. Chou and J. T. Hougen, *J. Chem. Phys.* **124**, 074319 (2006).

[167] N. D. Sanders, *J. Mol. Spectrosc.* **86**, 27 (1981).

[168] Y. Zhao, H. V. L. Nguyen, W. Stahl, J. T. Hougen, *J. Mol. Spectrosc.* **318**, 91 (2015).

[169] C. Cabezas, M. Varela, W. Caminati, S. Mata, J. C. López, J. L. Alonso, *J. Mol. Spectrosc.* **268**, 42 (2011).

[170] N. A. Seifert, I. A. Finneran, C. Perez, D. P. Zaleski, J. L. Neill, A. L. Steber, R. D. Suenram, A. Lesarri, S. T. Shipman, B. H. Pate, *J. Mol. Spectrosc.* **312**, 13 (2015).

[171] B. J. Drouin, J. C. Pearson, A. Walters, V. Lattanzi, *J. Mol. Spectrosc.* **240**, 227 (2006).

[172] K. Eibl, R. Kannengießer, W. Stahl, H.V.L. Nguyen, I. Kleiner, *Mol. Phys.* **114**, 3483 (2016).

[173] H. V. L. Nguyen, A. Jabri, V. Van, W. Stahl, *J. Phys. Chem. A* **118**, 12130 (2014).

[174] R. Kannengießer, M.J. Lach, W. Stahl, H.V.L. Nguyen, *ChemPhysChem* **16**, 1906 (2015).

[175] D. Jelisavac, D.C. Cortés-Gómez, H.V.L. Nguyen, L.W. Sutikdja, W. Stahl, I. Kleiner, *J. Mol. Spectrosc.* **257**, 111 (2009).

[176] (a) I. Kleiner, J. T. Hougen, R. D. Suenram, F. J. Lovas, M. Godefroid, *J. Mol. Spectrosc.* **153**, 578 (1992); (b) S. P. Belov, M. Yu. Tretyakov, I. Kleiner, J. T. Hougen, *J. Mol. Spectrosc.* **160**, 61 (1993); (c) I. Kleiner, F. J. Lovas, M. Godefroid, *J. Phys. Chem.* **25**, 1113 (1996).

[177] I. Kleiner, J. T. Hougen, J.-U. Grabow, S. P. Belov, M. Y. Tretyakov, J. Cosleou, *J. Mol. Spectrosc.* **179**, 41 (1996).

[178] V. V. Ilyushin, E. A. Alekseev, S. F. Dyubko, S. V. Podnos, I. Kleiner, L. Margulès, G. Wlodarczak, J. Demaison, J. Cosléou, B. Maté, E. N. Karyakin, G. Y. Golubiatnikov, G. T. Fraser, R. D. Suenram, J. T. Hougen, *J. Mol. Spectrosc.* **205**, 286 (2001).

[179] V. V. Ilyushin, E. A. Alekseev, S. F. Dyubko, I. Kleiner, *J. Mol. Spectrosc.* **220**, 170 (2003).

[180] M. Carvajal, L. Margulès, B. Tercero, K. Demyk, I. Kleiner, J. C. Guillemin, V. Lattanzi, A. Walters, J. Demaison, G. Wlodarczak, T. R. Huet, H. Møllendal, V. V. Ilyushin, J. Cernicharo, *Astron. Astrophys.* **500,** 1109 (2009).

[181] K. P. R. Nair, M. K. Jahn, A. Lesarri, V. V. Ilyushin and J.-U. Grabow, *Phys. Chem. Chem. Phys.* **17**, 26463 (2015).

[182] V. Ilyushin, *J. Mol. Spectrosc.* **345**, 64 (2018).

[183] A. Belloche, A. A. Meshcheryakov, R. T. Garrod, V. V. Ilyushin, E. A. Alekseev, R. A. Motiyenko, L. Margulès, H. S. P. Müller, and K. M. Menten, *Astron. Astrophys.* **601**, A49 (2017).

[184] R. Kannengießer, W. Stahl, H. V. L. Nguyen, I. Kleiner, *J. Phys. Chem. A* **120**, 3992 (2016).

[185] V. Van, T. Nguyen, W. Stahl, H.V.L. Nguyen, I. Kleiner, *J. Mol. Struct.* **1207**, 127787 (2020).

[186] A. Roucou, I. Kleiner, M. Goubet, S. Bteich, G. Mouret, R. Bocquet, F. Hindle, W. L. Meerts, A. Cuisset, *ChemPhysChem* **19**, 1056 (2018).

[187] P. Groner, S. Albert, E. Herbst, F. C. De Lucia, *Astrophys. J.* **500**, 1059 (1998).

[188] C. P. Endres, B. J. Drouin, J. C. Pearson, H. S. P. Müller, F. Lewen, S. Schlemmer, T. F. Giesen, *Astron. Astrophys.* **504**, 635 (2009).

[189] P. Groner, M. Winnewisser, I. R. Medvedev, F. C. De Lucia, E. Herbst, K. V. L. N. Sastry, *Astrophys. J. Suppl. Ser.* **169**, 28 (2007).

[190] Z. Kisiel, L. Pszczólkowski, E. Bialkowska-Jaworska, S. B. Charnley, *J. Mol. Spectrosc.* **241**, 220 (2007).

[191] A. Maeda, F. C. De Lucia, E. Herbst, *J. Mol. Spectrosc.* **251**, 293 (2008).

[192] A. Krasnicki, L. Pszczólkowski, Z. Kisiel, *J. Mol. Spectrosc.* **260**, 57 (2010).

[193] Y. Zhao, W. Stahl, H.V.L. Nguyen, *Chem. Phys. Lett.* **545**, 9 (2012).

[194] I. A. Armieieva, V. V. Ilyushin, E. A. Alekseev, O. A. Dorovskaya, L. Margulès, R. A. Motiyenko, *Radio Phys. Radio Astron.* **21**, 37 (2016).

[195] N. Ohashi, J. T. Hougen, R. Suenram, F. J. Lovas, Y. Kawashima, M. Fujitake, J. Pyka, *J. Mol. Spectrosc.* **227**, 28 (2004).

[196] V. Van, Dissertation, RWTH Aachen University (2017).

[197] L. Sutikdja, W. Stahl, V. Sironneau, H. V. L. Nguyen, I. Kleiner, *Chem. Phys. Lett.* **663**, 145 (2016).

[198] T. Attig, L. W. Sutikdja, R. Kannengießer, I. Kleiner, W. Stahl, *J. Mol. Spectrosc.* **284–285**, 8 (2013).

[199] T. Attig, R. Kannengießer, I. Kleiner, W. Stahl, *J. Mol. Spectrosc.* **290**, 24 (2013).

[200] T. Attig, R. Kannengießer, I. Kleiner, W. Stahl, *J. Mol. Spectrosc.* **298**, 47 (2014).

[201] H. Mouhib, D. Jelisavac, W. Stahl, R. Wang, I. Kalf, U. Englert, *ChemPhysChem* **12**, 761 (2011).

[202] L. W. Sutikdja, D. Jelisavac, W. Stahl, I. Kleiner, *Mol. Phys.* **110**, 2883 (2012).

[203] A. Jabri, V. Van, H. V. L. Nguyen, W. Stahl, I. Kleiner, *ChemPhysChem* **17**, 2660 (2016).

[204] L. Ferres, Dissertation, RWTH Aachen University (2019).

[205] R. M. Pitzer, *Acc. Chem. Res.* **16**, 207 (1983).

[206] S. Herbers, D. Wachsmuth, D. A. Obenchain, J.-U. Grabow, *J. Mol. Spectrosc.* **343**, 96 (2018).

[207] V. V. Ilyushin, E. A. Alekseev, S. F. Dyubko, I. Kleiner, J. T. Hougen, *J. Mol. Spectrosc.* **227**, 115 (2004).

[208] R. Kannengießer, Dissertation, RWTH Aachen University (2017).

[209] P. H. Turner, M. J. Corkill, A. P. Cox, *J. Phys. Chem. A* **83**, 1473 (1979).

[210] H. D. Rudolph and A. Trinkaus, *Z. Naturforsch.* **23a**, 68 (1968).

[211] P. R. Bunker and H. C. Longuet-Higgins, *Proc. R. Soc. A* **280**, 340 (1964).

[212] J. Nakagawa, M. Hayashi, Y. Endo, S. Saito, E. Hirota, *J. Chem. Phys.* **80**, 5922 (1984).

[213] J. Nakagawa, K. Yamada, M. Bestera, G. Winnerwisser, *J. Mol. Spectrosc.* **110**, 74 (1985).

[214] V. Ilyushin, R. Rizzato, L. Evangelisti, G. Feng, A. Maris, S. Melandri, W. Caminati, *J. Mol. Spectrosc.* **267**, 186 (2011).

[215] K. D. Hensel and M. C. L. Gerry, *J. Chem. Soc. Faraday Trans.* **90**, 3023 (1994).

[216] R. Subramanian, S. E. Novick, R. K. Bohn, *J. Mol. Spectrosc.* **222**, 57 (2003).

[217] V. M. Stolwijk and B. P. van Eijck, *J. Mol. Spectrosc.* **124**, 92 (1987).

[218] K. Eibl, Dissertation, RWTH Aachen University (2019).

[219] K. Eibl, W. Stahl, I. Kleiner, H. V. L. Nguyen, *J. Chem. Phys.* **149**, 144306 (2018).

[220] M. Andresen, I. Kleiner, M. Schwell, W. Stahl, H. V. L. Nguyen, *J. Phys. Chem. A* **122**, 7071 (2018).

[221] M. Andresen, I. Kleiner, M. Schwell, W. Stahl, H. V. L. Nguyen, *ChemPhysChem* **20**, 2063 (2019).

[222] M. Andresen, I. Kleiner, M. Schwell, W. Stahl, H. V. L. Nguyen, *J. Phys. Chem. A* **124**, 1353 (2020).

[223] Y. Zhao, J. Jin, W. Stahl, I. Kleiner, *J. Mol. Spectrosc.* **281**, 4 (2012).

[224] L. Tulimat, H. Mouhib, I. Kleiner, W. Stahl, *J. Mol. Spectroc.* **312**, 46 (2015).

[225] H.V.L. Nguyen, H. Mouhib, S. Klahm, W. Stahl, I. Kleiner, *Phys. Chem. Chem. Phys.* **15**, 10012 (2013).

[226] B. Reinhold, I. A. Finneran, S. T. Shipman, *J. Mol. Spectrosc.* 270, 89 (2011).

[227] L. Ferres, H. Mouhib, W. Stahl, M. Schwell, H.V.L. Nguyen, *J. Mol. Spectrosc.* **337**, 59 (2017).